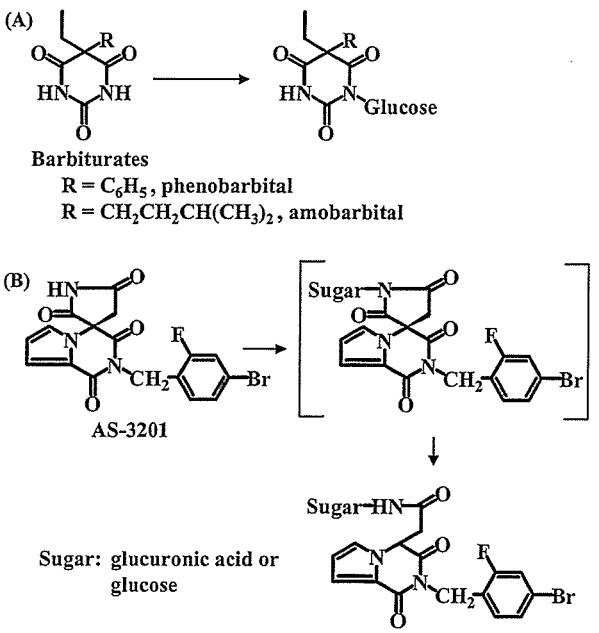

Fig. 1. *N*-Glucosidation of barbiturates (A) and AS-3201 (B) in humans.

the *N*-glucosides of barbiturates have been reported as the major urinary metabolites in humans (Fig. 1A), whereas the *N*-glucuronides have not been detected in human urine [7,8,10,11]. Thus, it was theorized that the enzyme(s) involved in barbiturate *N*-glucosidation might specifically utilize UDP-glucose as a sugar donor. However, to date, this enzyme(s) has not yet been clarified.

(*R*)-(−)-2-(4-bromo-2-fluorobenzyl)-1,2,3,4-tetrahydropyrrolo[1,2-*a*]pyrazine-4-spiro-3′-pyrrolidine-1,2′,3,5′-tetrone (AS-3201, Fig. 1B) is a structurally novel and potent aldose reductase inhibitor containing a succinimide ring [12,13]. The nitrogen atom in the succinimide ring is located between carbonyl groups, which is particularly similar to the target nitrogen atom for the glucosidation of barbiturates. *N*-Glucuronide and *N*-glucoside have been isolated and identified as the major metabolites of AS-3201 in humans, and it has been clarified that these conjugates formed through unstable intermediates [14].

In this paper, the enzyme(s) involved in the AS-3201 *N*-glucosidation was investigated, and compared with the enzyme(s) involved in the *N*-glucuronidation. We found that UGT2B enzymes catalyzed the *N*-glucosidation but not the *N*-glucuronidation of this chemical. Also, an application of RAF for recombinant human UGTs is reported for the first time.

2. Materials and methods

2.1. Materials

AS-3201 and [^{14}C]AS-3201 (1.41 MBq/mg) were synthesized at Dainippon Pharmaceutical. The radiochemical purity of [^{14}C]AS-3201 was more than 98%. Amobarbital, bilirubin, estradiol, estradiol 3-glucuronide, trifluoperazine, 4-methylumbelliferone, 4-nitrophenol, hyodeoxycholic acid, and azidothymidine were obtained from Sigma. UDP-GA and UDP-glucose were purchased from Wako Pure Chemical, recombinant UGTs (human UGT supersomes) and control microsomes (insect cell control supersomes) from Gentest, and pooled human liver microsomes (H0610) and human liver microsomes prepared from 16 individual donors from Xenotech. *cis*-4-Hydroxytamoxifen was kindly provided from Dr. Shinya Shibutani of State University of New York at Stony Brook, Stony Brook, NY. All other reagents and chemicals were of the highest grade commercially available.

2.2. Assays for AS-3201 N-glucuronidation and N-glucosidation

To determine enzyme activities for the AS-3201 *N*-glucosidation and *N*-glucuronidation, a reaction mixture (200 μL final volume) containing 0.1 M Tris–HCl (pH 7.1), 10 mM $MgCl_2$, 0.5 mg/mL of human liver microsomes or recombinant UGTs, UDP-glucose or UDP-GA, and AS-3201 or [^{14}C]AS-3201 was incubated at 37° for 2 hr. The incubation was performed using native human liver microsomes or UGT supersomes without activation by a detergent or alamethicin. Enzyme kinetic parameters were determined using AS-3201 and co-factors at concentrations of 25–500 and 50–2000 μM, respectively. The reaction was terminated by adding 50 μL of acetonitrile. After centrifugation at 15,000 *g* for 5 min, aliquots of the supernatant were subjected to HPLC or LC/MS. HPLC separations were performed using a Model 1100 liquid chromatograph system (Agilent) equipped with an Inertsil ODS-3V column (5 μm, 4.6 mm × 250 mm; GL-Science), maintained at 40°. The mobile phase consisted of solution A (10 mM ammonium acetate) and solution B (acetonitrile). At a constant flow rate (1 mL/min), a linear gradient from 15 to 60% of solution B was run over 35 min. The compounds were detected by radioactivity or absorbance at 296 nm. Radioactivity was counted by a flow-scintillation detector, FLO-ONE/Beta A-515 (Packard) using Ultima Flo-M (flow late, 2 mL/min; Packard) as a scintillation cocktail. The metabolites were quantified from the ratio of the peak radioactivity to the whole radioactivity eluted during the run time. LC/MS analysis was performed using a Model 1100 LC/MSD system (Agilent). Chromatographic separation was achieved with a Develosil ODS-UG5 column (2.0 mm × 100 mm; Nomura Chemical), maintained at 40°, using a two-solvent gradient system: solvent A (10 mM ammonium acetate) and solvent B (acetonitrile). At a constant flow rate (0.2 mL/min), a linear gradient from 15 to 55% of solvent B was run over 20 min. The mass spectrometer, with an ESI source, was operated in full scan mass spectrometry using the gas temperature of 320°, capillary voltage of 3.5 kV, and fragmentor of 75 in negative ion mode.

2.3. Amobarbital N-glucosidation assay

Amobarbital *N*-glucosyltransferase activity was assayed under the following conditions. The reaction mixture contained 0.1 M Tris–HCl (pH 7.1), 10 mM $MgCl_2$, 0.5 mg/mL of human liver microsomes, 2 mM UDP-glucose, and 50 μM amobarbital in a final volume of 200 μL. All reactions were conducted at 37° for 2 hr, and were terminated by adding 50 μL of acetonitrile. After centrifugation at 15,000 *g* for 5 min, aliquots of the supernatant were subjected to HPLC. HPLC was performed according to the method of Soine and Soine [15].

2.4. Other enzyme assays

Bilirubin glucuronyltransferase activity was determined by the method of Raijmakers *et al.* [16], 4-nitrophenol *O*-glucuronyltransferase and 4-methylumbelliferone *O*-glucuronyltransferase activities by the method of Hanioka *et al.* [17], azidothymidine *O*-glucuronyltransferase activity by the method of Sim *et al.* [18], and *cis*-4-hydroxytamoxifen *O*-glucuronyltransferase activity by the method of Nishiyama *et al.* [19]. The activities of estradiol 3-glucuronyltransferase and trifluoperazine *N*-glucuronyltransferase were determined according to the manufacturer's instructions for human UGT1A3 and UGT1A4 supersomes (Gentest). The concentrations of bilirubin, 4-nitrophenol, 4-methylumbelliferone, azidothymidine, *cis*-4-hydroxytamoxifen, estradiol, and trifluoperazine were 25, 100, 25, 250, 5, 10, and 125 μM, respectively. Hyodeoxycholic acid glucuronyltransferase activity was assayed in a reaction mixture containing 0.1 M Tris–HCl (pH 7.4), 10 mM $MgCl_2$, 0.25 mg/mL of human liver microsomes, 2 mM UDP-GA, and 15 μM hyodeoxycholic acid in a final volume of 200 μL. The reactions were conducted at 37° for 15 min, and were terminated by addition of acetonitrile (50 μL). After centrifugation at 15,000 *g* for 5 min, aliquots of the supernatant were subjected to LC/MS. LC/MS analysis was performed using a Model 1100 LC/MSD system (Agilent). Chromatographic separation was achieved with a Develosil ODS-UG5 column (2.0 mm × 100 mm; Nomura Chemical), maintained at 40°, using a two-solvent gradient system: solvent A (10 mM ammonium acetate) and solvent B (acetonitrile). At a constant flow rate (0.2 mL/min), a linear gradient from 20 to 40% of solvent B was run over 15 min. The mass spectrometer with an ESI source was operated at the gas temperature of 320°, capillary voltage of 4 kV, and fragmentor of 175 in negative ion mode. Hyodeoxycholic acid glucuronide was detected at selected ion monitoring (*m/z* 567). Radominska *et al.* [20] have clarified that 6-*O*-glucuronide of hyodeoxycholic acid is formed in human liver microsomes. Therefore, the glucuronide formed in this condition is considered to be hyodeoxycholic acid 6-*O*-glucuronide.

To determine the apparent K_m values of glucuronidation towards these substrates, several concentrations of the substrates (10–250 μM for bilirubin, 4-methylumbelliferone, and hyodeoxycholic acid; 5–100 μM for estradiol and *cis*-4-hydroxytamoxifen; 25–500 μM for trifluoperazine and 4-nitrophenol; and 100–2500 μM for azidothymidine) were incubated with pooled human liver microsomes. The K_m value was determined using least-squares nonlinear regression analysis by plotting the metabolite formation rates against the substrate concentrations.

2.5. Determination of RAF values

The RAF is a parameter to estimate the activity of the enzyme in its native environment from the activity of the cDNA expressed enzyme, and was originally suggested for CYPs [21]. This value can be calculated by applying Eq. (1).

$$\mathrm{RAF} = \frac{\text{enzyme activity in human liver microsomes}}{\text{enzyme activity in cDNA expressed enzyme}} \quad (1)$$

The RAF of a recombinant CYP enzyme has been determined by the method of Crespi [21] using a specific enzyme activity for the CYP isoform. The UGTs, however, exhibit overlapping substrate specificities and the substrates are generally catalyzed by multiple UGT isoforms [6,21]. Thus, the RAF for recombinant UGT enzymes could not be determined using the method of Crespi [21]. In this study, the RAF for UGT was therefore determined on the following basis. When the RAF and the enzyme activity of a recombinant UGT isoform are represented as $\mathrm{RAF_{UGT}}$ and $\mathrm{ACT_{UGT}}$, respectively, the enzyme activity of the UGT isoform in human liver microsomes can be represented by Eq. (2).

$$\mathrm{RAF_{UGT}} \times \mathrm{ACT_{UGT}} = (\text{enzyme activity of a UGT isoform in human liver microsomes}) \quad (2)$$

The sum of the enzyme activity of each UGT isoform expressed in human liver microsomes is conceivable as the total UGT activity in human liver microsomes. Therefore, the UGT activity in human liver microsomes can be represented by Eq. (3).

$$\sum(\mathrm{RAF_{UGT}} \times \mathrm{ACT_{UGT}}) = (\text{UGT activity in human liver microsomes}) \quad (3)$$

We employed bilirubin, estradiol, trifluoperazine, 4-methylumbelliferone, 4-nitrophenol, hyodeoxycholic acid, azidothymidine, and *cis*-4-hydroxytamoxifen as substrates to determine the RAF of recombinant UGT1A1, UGT1A3, UGT1A4, UGT1A6, UGT1A9, UGT2B4, UGT2B7, and UGT2B15. The substitution of glucuronyltransferase activities towards these substrates in each recombinant UGT isoform to Eq. (3) lead to the use of eight equations containing the RAF for these recombinant UGT isoforms. The RAF values of recombinant UGT isoforms were obtained as the solutions of the equations, by substituting in the appropriate $\mathrm{ACT_{UGT}}$ values determined in this study.

2.6. Statistical analysis

Multiple linear regression, least-squares regression, and least-squares nonlinear regression were performed using the Origin 7J software (OriginLab).

3. Results

3.1. AS-3201 N-glucosidation in human liver microsomes

The formation of AS-3201 *N*-glucuronide and *N*-glucoside was detectable after incubation of AS-3201 with human liver microsomes in the presence of UDP-GA or UDP-glucose (Fig. 2A and B). The retention times of AS-3201 *N*-glucuronide and *N*-glucoside were 13.0 and 15.8 min, respectively. Peaks of *m/z* 568, 570, 604, and 606 were detected in the LC/MS spectrum of the *N*-glucuronide (Fig. 2C). The peaks of *m/z* 568 and 570, or 604 and 606 are isotopic clusters. The peaks of *m/z* 568 and 570 were considered to be derived from $[M - H]^-$, and

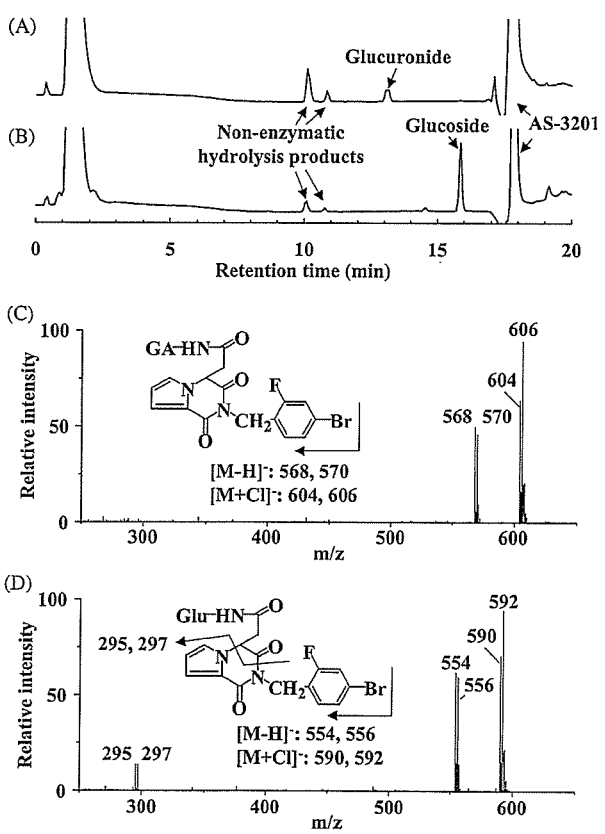

Fig. 2. HPLC chromatograms for the formation of AS-3201 *N*-glucuronide (A) and *N*-glucoside (B) monitored by absorbance at 296 nm. ESI-mass spectra of AS-3201 *N*-glucuronide (C) and *N*-glucoside (D) in the negative ionization mode. AS-3201 was incubated with pooled human liver microsomes in the presence of UDP-GA or UDP-glucose. The $[M - H]^-$ ions at *m/z* 568 and 570 or *m/z* 554 and 556 corresponded to AS-3201 *N*-glucuronide or *N*-glucoside, respectively. GA, glucuronic acid; Glu, glucose.

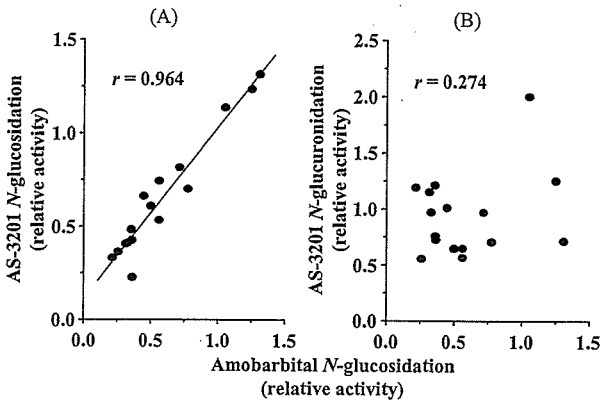

Fig. 3. Relationship between amobarbital *N*-glucosidation activities and activities for AS-3201 *N*-glucosidation (A) or *N*-glucuronidation (B) in human liver microsomes prepared from 16 individuals. Each enzyme activity was calculated from the HPLC peak area of each metabolite, and was represented relative to those with pooled human liver microsomes. The AS-3201 concentration was set at 37.5 μM for *N*-glucosidation and 125 μM for *N*-glucuronidation. Significant correlation between amobarbital *N*-glucosidation activity and AS-3201 *N*-glucosidation activity was observed ($r = 0.964$, $P < 0.01$).

m/z 604 and 606 from $[M + Cl]^-$ of the *N*-glucuronide. For *N*-glucoside, peaks of *m/z* 295, 297, 554, 556, 590, and 592 were detected in the LC/MS spectrum (Fig. 2D). The peaks of *m/z* 554 and 556 were considered to be derived from $[M - H]$, and *m/z* 590 and 592 from $[M + Cl]^-$ of the *N*-glucoside. The peaks of *m/z* 295 and 297 were considered to be the fragment ions derived from the *N*-glucoside, since they were also observed in the LC/MS spectrum of the aglycone (data not shown).

The enzyme activities for AS-3201 *N*-glucosidation and *N*-glucuronidation were determined with human liver microsomes prepared from sixteen individuals, and were compared with those for amobarbital *N*-glucosidation (Fig. 3). Relative enzyme activities for amobarbital *N*-glucosidation were highly correlated with those for AS-3201 *N*-glucosidation ($r = 0.964$, $P < 0.01$) but not with those for AS-3201 *N*-glucuronidation ($r = 0.274$). These results probably indicate that the *N*-glucosidation of AS-3201 and amobarbital are catalyzed by the same enzyme(s).

To determine kinetic parameters with respects to the concentration of the substrate and co-factors, various concentrations of [^{14}C]AS-3201 and either UDP-GA or UDP-glucose were incubated with pooled human liver microsomes. The enzyme activities were estimated by determining the radioactivity of each conjugate, as described in Section 2. The kinetic parameters for AS-3201 and co-factors were summarized in Table 1. The K_m values for AS-3201 and co-factor in the *N*-glucosidation were 75.3 and 392 μM, respectively. These values were almost three times lower than those in *N*-glucuronidation, suggesting that the affinities of the substrate and the co-factor to UGT protein(s) for the *N*-glucosidation were higher than those for *N*-glucuronidation.

Table 1
Kinetic parameters for glucosidation and glucuronidation of AS-3201 by human liver microsomes

	Substrate			Co-factor		
	K_m (μM)	V_{max} (nmol/hr/mg)	V_{max}/K_m (mL/hr/mg)	K_m (μM)	V_{max} (nmol/hr/mg)	V_{max}/K_m (mL/hr/mg)
Glucosidation	75.3	7.58	0.101	392	4.76	0.012
Glucuronidation	242	1.08	0.004	1320	0.84	0.001

The concentration of co-factors was fixed at 2 mM to determine the kinetic parameters towards AS-3201. The concentration of AS-3201 was fixed at 50 μM (*N*-glucosidation) or 200 μM (*N*-glucuronidation) to determine the kinetic parameters towards the UDP-GA or the UDP-glucose.

3.2. Determination of RAF for recombinant UGT isoforms

The K_m values of glucuronidation towards eight substrates in human liver microsomes were determined (Table 2). It was shown that the concentrations of the substrates employed in this study were lower than the K_m towards the substrates in human liver microsomes. Therefore, the enzyme activities observed under these conditions are in proportion to the intrinsic clearance of the reactions. It has been reported that the RAF calculated using the intrinsic clearance is the most appropriate value to estimate the activity of the enzyme in its native environment from the activity of the cDNA expressed enzyme [23].

Relative enzyme activities in each recombinant UGT isoform and pooled human liver microsomes are shown in Fig. 4. The glucuronyltransferase activities towards bilirubin and trifluoperazine were detectable with UGT1A1 and UGT1A4, respectively. The glucuronyltransferase activities towards other substrates were detectable with multiple UGT isoforms. When the activities of pooled human liver microsomes were defined as one, the substitution of these enzyme activities to Eq. (3) led to the following Eqs. (4)–(11).

$$RAF_{UGT1A1} \times 3.19 = 1 \quad (4)$$

$$(RAF_{UGT1A1} \times 3.09) + (RAF_{UGT1A3} \times 0.33) = 1 \quad (5)$$

$$RAF_{UGT1A4} \times 2.59 = 1 \quad (6)$$

$$(RAF_{UGT1A1} \times 0.02) + (RAF_{UGT1A6} \times 0.99) + (RAF_{UGT1A9} \times 0.52) + (RAF_{UGT2B15} \times 0.04) = 1 \quad (7)$$

$$(RAF_{UGT1A1} \times 0.01) + (RAF_{UGT1A3} \times 0.01) + (RAF_{UGT1A6} \times 2.00) + (RAF_{UGT1A9} \times 0.30) + (RAF_{UGT2B7} \times 0.06) = 1 \quad (8)$$

$$(RAF_{UGT2B4} \times 0.05) + (RAF_{UGT2B7} \times 1.64) = 1 \quad (9)$$

$$(RAF_{UGT2B4} \times 0.08) + (RAF_{UGT2B7} \times 1.50) = 1 \quad (10)$$

$$(RAF_{UGT1A1} \times 0.01) + (RAF_{UGT1A3} \times 0.01) + (RAF_{UGT2B7} \times 0.08) + (RAF_{UGT2B15} \times 0.17) = 1 \quad (11)$$

The RAF values for recombinant UGT enzymes were obtained as the solutions of these equations (Table 2). The RAF values for UGT1A1, UGT1A3, UGT1A4, UGT1A6, UGT1A9, and UGT2B7 were lower than one, indicating that the activities of these recombinant UGT enzymes are higher than the activities in their native environment. On the other hand, the RAF values for UGT2B4 and UGT2B15 were 2.18 and 5.60, respectively.

Table 2
Relative glucuronosyltransferase activities towards eight substrates and the RAF value for each recombinant UGT isoform

	Substrate								RAF
	BIL	EST	TFP	MU	NP	HDC	AZT	OHT	
K_m (μM)	48.2	14.1	247	66.6	184	26.8	1550	8.74	
Substrate concentration (μM)	25	10	125	25	100	15	250	5	
UGT1A1	3.19	3.09	–	0.02	0.01	–	–	0.01	0.31
UGT1A3	–	0.33	–	–	0.01	–	–	0.01	0.09
UGT1A4	–	–	2.59	–	–	–	–	–	0.39
UGT1A6	–	–	–	0.99	2.00	–	–	–	0.36
UGT1A9	–	–	–	0.52	0.30	–	–	–	0.79
UGT2B4	–	–	–	–	–	0.05	0.08	–	2.18
UGT2B7	–	–	–	–	0.06	1.64	1.50	0.08	0.55
UGT2B15	–	–	–	0.04	–	–	–	0.17	5.60

Each enzyme activity represents relative activity to the activity obtained with pooled human liver microsomes. The definition of RAF was described in Section 2. The K_m values of glucuronidation towards these substrates with human liver microsomes are shown. BIL, bilirubin; EST, estradiol; TFP, trifluoperazine; MU, 4-methylumbelliferone; NP, 4-nitrophenol; HDC, hyodeoxycholic acid; AZT, azidothymidine; OHT, *cis*-4-hydroxytamoxifen; –, not detectable.

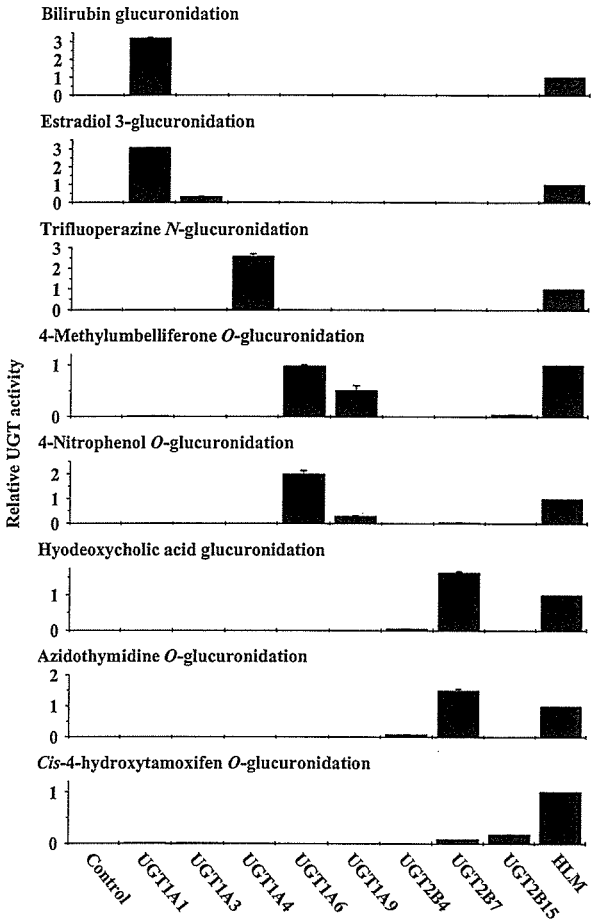

Fig. 4. Relative glucuronyltransferase activities towards eight substrates with each recombinant UGT isoform. Each activity was represented as the relative activity to the activity obtained with pooled human liver microsomes (mean ± SD, N = 3). Insect cell control supersomes were used as a control. HLM, pooled human liver microsomes.

3.3. UGT isoform(s) responsible for AS-3201 N-glucosidation

AS-3201 was incubated with recombinant UGT enzymes in the presence of UDP-glucose or UDP-GA. The substrate concentration was set at 37.5 μM for *N*-glucosidation and 125 μM for *N*-glucuronidation, both of which are almost a half of the K_m of *N*-glucosidation and *N*-glucuronidation in human liver microsomes. The enzyme activities observed under these conditions, therefore, are in proportion to the intrinsic clearance of the reactions. The *N*-glucosidation was detectable with UGT1A1, UGT1A3, UGT1A4, UGT2B4, UGT2B7, and UGT2B15 (Fig. 5A). The highest enzyme activity was seen with UGT1A4, followed by UGT2B15 and UGT1A3. These results indicate both UGT1A and UGT2B isoforms can catalyze AS-3201 *N*-glucosidation. On the other hand, the *N*-glucuronidations were detectable with UGT1A isoforms (UGT1A1, UGT1A3, UGT1A4, and UGT1A9) but not with UGT2B isoforms (Fig. 5B). Therefore, it appeared that UGT2B isoforms utilize UDP-glucose alone as a co-

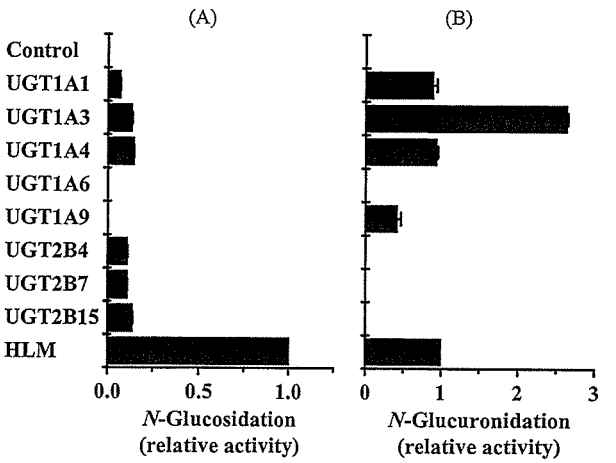

Fig. 5. Rate of AS-3201 *N*-glucosidation (A) and *N*-glucuronidation (B) catalyzed by recombinant UGT enzymes. Insect cell control supersomes were used as a control. The activity for each UGT isoform was represented as the relative activity to the activity obtained with pooled human liver microsomes (mean ± SD, N = 3). HLM, pooled human liver microsomes.

factor for AS-3201 conjugation. UGT1A8 and UGT1A10, which are expressed in extrahepatic tissues [24,25], catalyzed the *N*-glucosidation (data not shown).

To estimate the actual *N*-glucosyltransferase activity of each UGT isoform in human liver microsomes, the *N*-glucosyltransferase activity in each recombinant UGT enzyme was corrected by the RAF determined in this study (Fig. 6A). The highest enzyme activity was seen with UGT2B15, followed by UGT2B4 and UGT2B7. The enzyme activity in UGT1A isoforms was relatively low. These results show that UGT2B isoforms are mainly responsible for AS-3201 *N*-glucosidation in human liver microsomes. The *N*-glucuronyltransferase activity of each recombinant UGT enzyme was also corrected by the RAF

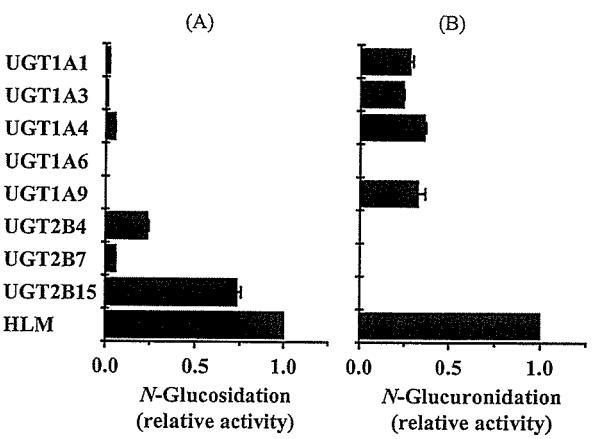

Fig. 6. Predicted rate of AS-3201 *N*-glucosidation (A) and *N*-glucuronidation (B) catalyzed by UGT isoforms in human liver microsomes. The predicted enzyme activities were determined using the RAF and the activities of recombinant UGT enzymes. The activity for each UGT isoform was represented as the relative activity to the activity obtained with pooled human liver microsomes (mean ± SD, N = 3). HLM, pooled human liver microsomes.

Table 3
The K_m (μM) of each UGT isoform for glucosidation and glucuronidation of AS-3201 by recombinant UGTs

	Glucosidation		Glucuronidation	
	AS-3201	UDP-glucose	AS-3201	UDP-GA
UGT1A1	158	648	293	1830
UGT1A3	109	627	320	1790
UGT1A4	315	1070	529	2420
UGT1A9	–	–	295	1550
UGT2B4	161	616	–	–
UGT2B7	148	513	–	–
UGT2B15	122	589	–	–

The concentration of co-factors (UDP-glucose and UDP-GA) was fixed at 2 mM to determine the K_m towards the AS-3201. The concentration of AS-3201 was fixed at 50 μM (*N*-glucosidation) or 200 μM (*N*-glucuronidation) to determine the K_m towards the UDP-GA or the UDP-glucose.

(Fig. 6B). The result shows that the actual *N*-glucuronyltransferase activity of UGT1A1, UGT1A3, UGT1A4, and UGT1A9 isoforms is nearly the same in human liver microsomes.

The K_m values of each recombinant UGT for the substrate (AS-3201) and the co-factors (UDP-glucose and UDP-GA) in the *N*-glucosidation of AS-3201 were determined (Table 3). The K_m values for both the substrate and the co-factors varied. However, the variation was within three times or less between the UGT1A and the UGT2B isoforms. In addition, the variation of the K_m values in the *N*-glucuronidation was within two times or less among the UGT1A isoforms. Therefore, the affinities of the substrate and the co-factors to the UGT protein were nearly the same among the UGT isoforms.

The enzyme activities for AS-3201 *N*-glucosidation in human liver microsomes prepared from sixteen individual subjects were compared with those for azidothymidine *O*-glucuronidation and *cis*-4-hydroxytamoxifen *O*-glucuronidation (Fig. 7). These enzyme activities were likely to be derived from UGT2B isoforms as shown in Table 2. A multivariate linear regression analysis showed that enzyme activities for AS-3201 *N*-glucosidation was significantly correlated with those for azidothymidine *O*-glucuronidation and *cis*-4-hydroxytamoxifen *O*-glucuronidation ($r = 0.750$, $P < 0.01$). Additionally, enzyme activities for amobarbital *N*-glucosidation were significantly correlated with those for azidothymidine *O*-glucuronidation and *cis*-4-hydroxytamoxifen *O*-glucuronidation ($r = 0.784$, $P < 0.01$, data not shown).

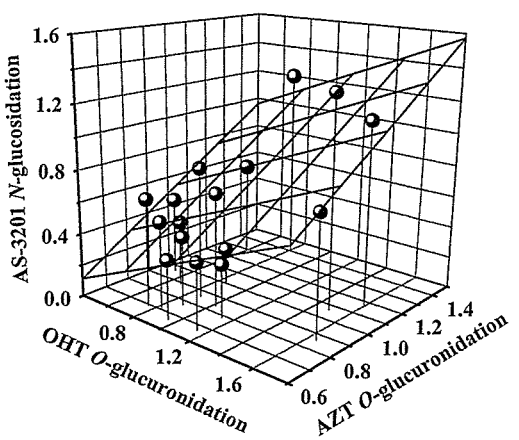

Fig. 7. Correlation among the activity of AS-3201 *N*-glucosidation and the activities of *cis*-4-hydroxytamoxifen (OHT) *O*-glucuronidation and azidothymidine (AZT) *O*-glucuronidation. A multivariate linear regression analysis shows the significant correlation between AS-3201 *N*-glucosidation activity and activities for OHT *O*-glucuronidation and AZT *O*-glucuronidation ($r = 0.750$, $P < 0.01$). Each activity represents relative to the activity obtained with pooled human liver microsomes.

4. Discussion

In the present study, we described several lines of evidence that the UGT2B isoforms are responsible for AS-3201 *N*-glucosidation but not *N*-glucuronidation in human liver microsomes. Our results indicated that UGT2B15 mostly contributes to AS-3201 *N*-glucosidation in human liver microsomes. UGT2B15 is known to catalyze the glucuronidation of a number of steroids, including 5α-dihydrotestosterone and androstane-3α,17β-diol [26,27]. A polymorphism of the *UGT2B15* gene in the coding region that results in an amino acid change at residue 85 from Asp to Tyr has been reported [28]. This polymorphism altered glucuronyltransferase activities towards 5α-dihydrotestosterone and androstane-3α,17β-diol [28]. It has been reported that the *N*-glucosidation is one of the major metabolic pathways for amobarbital in humans [8]. Therefore, the genotype of the *UGT2B15* gene might affect the pharmacokinetics of amobarbital, as well as AS-3201, in humans.

The RAF provides a means to relate the activity of the cDNA-expressed enzyme to the activity of the enzyme in its native environment. This was first proposed for recombinant CYP enzymes [21]. So far, several groups have reported the RAF values for recombinant CYP enzymes [23,29–31], whereas no one has reported the RAF of recombinant UGT enzymes. In this study, we provided a novel strategy to determine the RAF of recombinant UGT enzymes. We conceived that the sum of the enzyme activity of UGT isoforms expressed in human liver microsomes is equal to the UGT activity of human liver microsomes. Actually, the sum of the enzyme activity of UGT isoforms corrected by the RAF was almost the same activity of human liver microsomes in both the *N*-glucosidation and the *N*-glucuronidation. These results suggest that the RAF value determined in this study is appropriate to estimate the enzyme activity of the UGT isoform in human liver microsomes from the activity of the recombinant UGT enzyme.

It was reported in the literature that human UGT1A1 could catalyze bilirubin glucosidation, as well as bilirubin glucuronidation [32]. We found that human UGT1A1 was also able to catalyze both the *N*-glucosidation and the *N*-

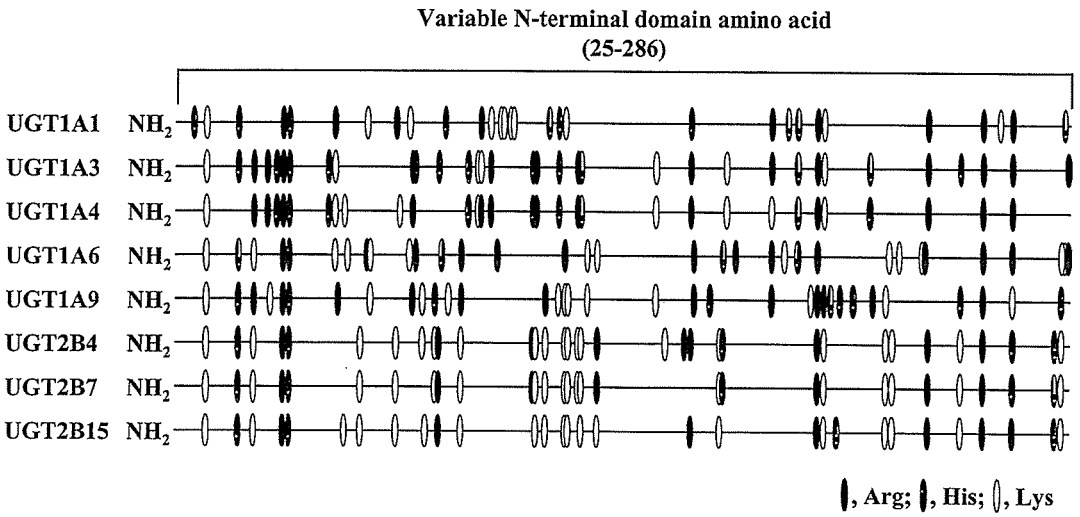

Fig. 8. Comparison of amino acid sequence in the N-terminal (25–286) of UGT proteins. The positions of Arg, His, and Lys residues for co-factor binding are shown.

glucuronidation of AS-3201. UGT1A3 and UGT1A4 are known as the UGT enzymes that catalyze a number of amine glucuronidations [33,34]. In this study, UGT1A3 and UGT1A4 catalyzed the AS-3201 *N*-glucosidation, as well as the AS-3201 *N*-glucuronidation, indicating these UGT1A isoforms as well as UGT1A1 utilize both UDP-glucose and UDP-glucuronic acid as a sugar donor for the conjugation of AS-3201. In contrast, UGT2B isoforms specifically utilize UDP-glucose, but not UDP-glucuronic acid, as a sugar donor for the conjugation of AS-3201. We then speculated that this property of UGT2B enzymes is determined by the amino acid sequence of UGT2B protein. The N-terminal and the C-terminal of the UGT protein contain an aglycone binding site and a transmembrane fragment, respectively [22]. Although UDP-sugar possibly interacts with both N- and C-terminal domains of the UGT protein, the carboxyl moiety of UDP-GA would interact with an Arg residue in the N-terminal [22,35]. In addition, the UDP moiety, which is common to UDP-sugar, would interact with the amino acid residue from 352 to 400 in the C-terminal. These findings suggest that the N-terminal sequence of UGT protein is important for the co-factor selective conjugation of AS-3201 by UGT2B. The amino acid sequence of the N-terminal is highly conserved among UGT2B proteins, but not between UGT1A and UGT2B proteins [1]. Arg residue for co-factor binding, as well as the other basic amino acid residues, locates itself on almost the same region in the UGT2B proteins (Fig. 8), suggesting that Arg residue interacting with the carboxyl moiety of UDP-GA is conserved in UGT2B proteins. Although the substrate possibly interacts with the C-terminal of UGT protein as well, the amino acid sequence of the C-terminal is highly conserved among UGT2B proteins. Therefore, the structure of the UGT2B protein and UGT2B protein–AS-3201 complex might be highly conserved among UGT2B isoforms, and the structure of UGT2B protein–AS-3201 complex might elucidate this enzyme property.

The difference between UDP-glucose and UDP-GA is only the C6 of the sugar moiety. However, the pK_a of glucose and glucuronic acid, calculated using the Pallas software (CompuDrug), were 15.6 and 2.65, respectively. This indicates that glucuronic acid, but not glucose, is ionized at physiological pH. Therefore, it is believed that the difference between UDP-glucose and UDP-GA judged with ionicity is one of the important determinants of co-factor selection for specific conjugation of AS-3201 by UGT2B enzymes.

Glucosidation is known as a metabolic reaction for a relatively limited number of compounds. Recently, it has been reported that an endothelin ETA receptor antagonist [36] and hyodeoxycholic acid [37] were conjugated with both glucuronic acid and glucose by UGT2B7 in human liver microsomes. These findings indicate that UGT2B7 can utilize both UDP-glucuronic acid and UDP-glucose as a sugar donor, and support the hypothesis that the structure of UGT2B enzyme–AS-3201 complex might elucidate the properties of UGT2B enzymes.

In conclusion, we showed evidence that UGT2B enzymes are involved in AS-3201 *N*-glucosidation, as well as amobarbital *N*-glucosidation, in human liver microsomes. These enzymes utilized UDP-glucose specifically, but not UDP-GA, as a sugar donor for the AS-3201 conjugation. Although the mechanism of this selectivity is not fully understood yet, it is believed that the tridimensional structure of UGT2B enzyme–AS-3201 complex might elucidate this enzyme property.

Acknowledgments

We thank Mr. Glen Argyle (Dainippon Pharmaceutical) for critical reading of the manuscript. This study was supported in part by a Grant-in-Aid (No. 99-2) from The Organization for Pharmaceutical Safety and Research

(OPSR), Ministry of Education, Science, Sports and Culture of Japan, and Ministry of Health, Labour and Welfare of Japan.

References

[1] Mackenzie PI, Owens IS, Burchell B, Bock KW, Bairoch A, Bélanger A, Fournel-Gigleux S, Green M, Hum DW, Iyanagi T, Lancet D, Louisot P, Magdalou J, Chowdhury JR, Ritter JK, Schachter H, Tephly TR, Tipton KF, Nebert DW. The UDP glycosyltransferase gene superfamily: recommended nomenclature update based on evolutionary divergence. Pharmacogenetics 1997;7:255–69.

[2] Owens IS, Ritter JK. Gene structure at the human *UGT1* locus creates diversity in isozyme structure, substrate specificity, and regulation. Prog Nucleic Acid Res Mol Biol 1995;51:305–38.

[3] Monaghan G, Clarke DJ, Povey S, See CG, Boxer M, Burchell B. Isolation of a human YAC contig encompassing a cluster of *UGT2* genes and its regional localization to chromosome 4q13. Genomics 1994;23:496–9.

[4] Turgeon D, Carrier JS, Lévesque E, Beatty BG, Bélanger A, Hum DW. Isolation and characterization of the human *UGT2B15* gene, localized within a cluster of *UGT2B* genes and pseudogenes on chromosome 4. J Mol Biol 2000;295:489–504.

[5] Bosma PJ, Seppen J, Goldhoorn B, Bakker C, Oude Elferink RP, Chowdhury JR, Chowdhury NR, Jansen PL. Bilirubin UDP-glucuronosyltransferase 1 is the only relevant bilirubin glucuronidating isoform in man. J Biol Chem 1994;269:17960–4.

[6] Tukey RH, Strassburg CP. Human UDP-glucuronosyltransferases: metabolism, expression, and disease. Annu Rev Pharmacol Toxicol 2000;40:581–616.

[7] Tang BK, Kalow W, Grey AA. Metabolic fate of phenobarbital in man. *N*-Glucoside formation. Drug Metab Dispos 1979;7:315–8.

[8] Tang BK, Kalow W, Grey AA. Amobarbital metabolism in man: *N*-glucoside formation. Res Commun Chem Pathol Pharmacol 1978;21:45–53.

[9] Ahmad B, Powell JW. N1-glucosides as urinary metabolites of sulphadimidine, sulphamerazine and sulphamethoxazole. Eur J Drug Metab Pharmacokinet 1988;13:177–83.

[10] Tang BK. Drug glucosidation. Pharmacol Ther 1990;46:53–6.

[11] Paibir SG, Soine WH. High-performance liquid chromatographic analysis of phenobarbital and phenobarbital metabolites in human urine. J Chromatogr B Biomed Sci Appl 1997;691:111–7.

[12] Negoro T, Murata M, Ueda S, Fujitani B, Ono Y, Kuromiya A, Komiya M, Suzuki K, Matsumoto J. Novel, highly potent aldose reductase inhibitors: (*R*)-(−)-2-(4-bromo-2-fluorobenzyl)-1,2,3,4-tetrahydropyrrolo[1,2-*a*]pyrazine-4-spiro-3′-pyrrolidine-1,2′,3,5′-tetrone (AS-3201) and its congeners. J Med Chem 1998;41:4118–29.

[13] Kurono M, Fujiwara I, Yoshida K. Stereospecific interaction of a novel spirosuccinimide type aldose reductase inhibitor, AS-3201, with aldose reductase. Biochemistry 2001;40:8216–26.

[14] Toide K, Matsushita H, Hashizume T, Terauchi Y, Fujii T. *In vitro* metabolism of aldose reductase inhibitor AS-3201 in human liver microsomes. Ninth North American ISSX Meeting, 1999 Oct 24–28; Nashville, TN, Abstract No. 155.

[15] Soine PJ, Soine WH. High-performance liquid chromatographic determination of the diastereomers of 1-(α-D-glucopyranosyl)amobarbital in urine. J Chromatogr 1987;422:309–14.

[16] Raijmakers MT, Jansen PL, Steegers EA, Peters WH. Association of human liver bilirubin UDP-glucuronyltransferase activity with a polymorphism in the promoter region of the UGT1A1 gene. J Hepatol 2000;33:348–51.

[17] Hanioka N, Jinno H, Tanaka-Kagawa T, Nishimura T, Ando M. Determination of UDP-glucuronosyltransferase UGT1A6 activity in human and rat liver microsomes by HPLC with UV detection. J Pharm Biomed Anal 2001;25:65–75.

[18] Sim SM, Back DJ, Breckenridge AM. The effect of various drugs on the glucuronidation of zidovudine (azidothymidine AZT) by human liver microsomes. Br J Clin Pharmacol 1991;32:17–21.

[19] Nishiyama T, Ogura K, Nakano H, Ohnuma T, Kaku T, Hiratsuka A, Muro K, Watabe T. Reverse geometrical selectivity in glucuronidation and sulfation of *cis*- and *trans*-4-hydroxytamoxifens by human liver UDP-glucuronosyltransferases and sulfotransferases. Biochem Pharmacol 2002;63:1817–30.

[20] Radominska A, Little J, Pyrek JS, Drake RR, Igari Y, Fournel-Gigleux S, Magdalou J, Burchell B, Elbein AD, Siest G, Lester R. A novel UDP-Glc-specific glucosyltransferase catalyzing the biosynthesis of 6-*O*-glucosides of bile acids in human liver microsomes. J Biol Chem 1993;268:15127–35.

[21] Crespi CL. Xenobiotic-metabolizing human cells as tools for pharmacological and toxicological research. Adv Drug Res 1995;26:179–235.

[22] Radominska-Pandya A, Czernik PJ, Little JM, Battaglia E, Mackenzie PI. Structural and functional studies of UDP-glucuronosyltransferases. Drug Metab Rev 1999;31:817–99.

[23] Nakajima M, Nakamura S, Tokudome S, Shimada N, Yamazaki H, Yokoi T. Azelastine *N*-demethylation by cytochrome P-450 (CYP)3A4, CYP2D6, and CYP1A2 in human liver microsomes: evaluation of approach to predict the contribution of multiple CYPs. Drug Metab Dispos 1999;27:1381–91.

[24] Strassburg CP, Oldhafer K, Manns MP, Tukey RH. Differential expression of the UGT1A locus in human liver, biliary, and gastric tissue: identification of *UGT1A7* and *UGT1A10* transcripts in extrahepatic tissue. Mol Pharmacol 1997;52:212–20.

[25] Strassburg CP, Manns MP, Tukey RH. Expression of the UDP-glucuronosyltransferase 1A locus in human colon. Identification and characterization of the novel extrahepatic UGT1A8. J Biol Chem 1998;273:8719–26.

[26] Green MD, Oturu EM, Tephly TR. Stable expression of a human liver UDPglucuronosyltransferase (UGT2B15) with activity towards steroid and xenobiotic substrates. Drug Metab Dispos 1994;22:799–805.

[27] Beaulieu M, Lévesque E, Hum DW, Bélanger A. Isolation and characterization of a novel cDNA encoding a human UDP-glucuronosyltransferase active on C_{19} steroids. J Biol Chem 1996;271:22855–62.

[28] Lévesque E, Beaulieu M, Green MD, Tephly TR, Bélanger A, Hum DW. Isolation and characterization of UGT2B15(Y85): a UDP-glucuronosyltransferase encoded by a polymorphic gene. Pharmacogenetics 1997;7:317–25.

[29] Fitzsimmons ME, Collins JM. Selective biotransformation of the human immunodeficiency virus protease inhibitor saquinavir by human small-intestinal cytochrome P4503A4: potential contribution to high first-pass metabolism. Drug Metab Dispos 1997;25:256–66.

[30] Stormer E, von Moltke LL, Greenblatt DJ. Scaling drug biotransformation data from cDNA-expressed cytochrome P-450 to human liver: a comparison of relative activity factors and human liver abundance in studies of mirtazapine metabolism. J Pharmacol Exp Ther 2000;295:793–801.

[31] Venkatakrishnan K, von Moltke LL, Court MH, Harmatz JS, Crespi CL, Greenblatt DJ. Comparison between cytochrome P450 (CYP) content and relative activity approaches to scaling from cDNA-expressed CYPs to human liver microsomes: ratios of accessory proteins as sources of discrepancies between the approaches. Drug Metab Dispos 2000;28:1493–504.

[32] Senafi SB, Clarke DJ, Burchell B. Investigation of the substrate specificity of a cloned expressed human bilirubin UDP-glucuronosyltransferase: UDP-sugar specificity and involvement in steroid and xenobiotic glucuronidation. Biochem J 1994;303:233–40.

[33] Green MD, Tephly TR. Glucuronidation of amines and hydroxylated xenobiotics and endobiotics catalyzed by expressed human UGT1.4 protein. Drug Metab Dispos 1996;24:356–63.

[34] Green MD, King CD, Mojarrabi B, Mackenzie PI, Tephly TR. Glucuronidation of amines and other xenobiotics catalyzed by expressed human UDP-glucuronosyltransferase 1A3. Drug Metab Dispos 1998;26:507–12.
[35] Zakim D, Hochman Y, Kenney WC. Evidence for an active site arginine in UDP-glucuronyltransferase. J Biol Chem 1983;258: 6430–4.
[36] Tang C, Hochman JH, Ma B, Subramanian R, Vyas KP. Acyl glucuronidation and glucosidation of a new and selective endothelin ET(A) receptor antagonist in human liver microsomes. Drug Metab Dispos 2003;31:37–45.
[37] Mackenzie P, Little JM, Radominska-Pandya A. Glucosidation of hyodeoxycholic acid by UDP-glucuronosyltransferase 2B7. Biochem Pharmacol 2003;65:417–21.

0090-9556/04/3204-376–378$20.00
DRUG METABOLISM AND DISPOSITION
Vol. 32, No. 4
1275/1138603
Printed in U.S.A.

DMD 32:376–378, 2004

Short Communication

CLONING CYP2D21 AND CYP3A22 CDNAS FROM LIVER OF MINIATURE PIGS

(Received September 5, 2003; accepted January 7, 2004)

This article is available online at http://dmd.aspetjournals.org

ABSTRACT:

To compare the identity of the primary structure of drug-metabolizing cytochrome P450 between miniature pigs and humans, two cDNA clones, coding for miniature pig CYP2D21 and CYP3A22, were isolated. The deduced amino acid sequences of CYP2D21 and CYP3A22 were 78.3 and 75.0% identical to human CYP2D6 and CYP3A4, respectively. These values were nearly the same as those of bovine, dog, and some rodent isoforms, and 12.2 to 18.4% lower than those of nonhuman primates such as cynomolgus monkeys, Japanese monkey, and marmosets. These data indicate that miniature pig P450s are genetically not so close as monkey P450s to human P450s as previously expected. The recombinant CYP2D21 enzyme, however, showed bufuralol 1′-hydroxylase activity, suggesting that miniature pig CYP2D21 is capable of metabolizing some of the same substrates associated with human CYP2D6 despite its low identity to human counterparts.

The miniature pig is small in size (~50 kg body weight in adult animals) and has been developed through selective breeding so as to override the shortcomings arising from the large body size of domestic pigs (Khan, 1984). The miniature pig is becoming a popular alternative to traditional nonrodent species in pharmacological and toxicological studies. Porcine hepatocytes continue to find increasing application in bioartificial liver devices (Watanabe et al., 1997). These uses are, in part, based on findings that many anatomical, physiological, and biochemical properties of domestic and miniature pigs are close to those of humans (Swindle and Smith, 1998). However, it has been well recognized that qualitative and quantitative species differences in drug-metabolizing systems are present among animal species including man (Caldwell, 1981). Thus, information on the primary structure of drug-metabolizing enzymes of experimental animal species and information on the identity of those enzymes between human and experimental animal species is important to explain species differences in drug-metabolizing systems and to predict drug metabolism in the human body. Genetic distance of some porcine genes to human orthologs has been clarified. Regarding porcine *CYP* genes, some forms of P450[1] concerned with endogenous metabolism such as CYP5A (accession no. L131128), CYP11B1 (D38590), CYP19 (U37311), CYP21 (M83939), and CYP51 (AB042975) have been isolated from domestic pigs. These forms shared amino acid sequence identities ranging from 73 to 95% to human orthologous genes. cDNA cloning of the entire coding sequence of two drug-metabolizing P450s, namely CYP2D25 and CYP3A29, from domestic pigs has been reported (Postlind et al., 1997; Nissen et al., 1998). Additionally, the partial sequences of cDNAs for five drug-metabolizing CYP2Cs (2C32, 2C33, 2C34, 2C35 and 2C42) from domestic pigs have been reported (Zaphiropoulos et al., 1995; Nissen et al., 1998). However, study of cDNA cloning from miniature pig has not yet been reported. The aims of the present study were to demonstrate in miniature pigs the primary structure of drug-metabolizing P450s, especially CYP3A and CYP2D, which are responsible for the metabolism of many prescribed drugs, and to compare these with those of human orthologs.

This work was supported in part by a grant-in-aid for Scientific Research from the Ministry of Education, Sciences, Culture and Sports of Japan.

[1] Abbreviations used are: P450, cytochrome P450; bp, base pairs; SRS, substrate recognition site.

Address correspondence to: Dr. Tsutomu Sakuma, Department of Toxicology, Faculty of Pharmaceutical Sciences, Toyama Medical and Pharmaceutical University, 2630 Sugitani, Toyama, Toyama 930-0194, Japan. E-mail: tsakuma@ms.toyama-mpu.ac.jp

Materials and Methods

Animals. Two 24-week-old male Göttingen miniature pigs of about 15 kg in body weight were used in this study. Livers were stored at −80°C until use for the preparation of RNA and microsomes. All experiments were performed in accordance with the Principles of Laboratory Animal Care (National Institutes of Health publication 85-23, revised 1985).

Construction and Screening of the Miniature Pig Liver cDNA Library. Poly(A)$^+$ RNA was prepared from the liver of an untreated male miniature pig by oligo(dT)-cellulose column chromatography. A cDNA library was constructed as described previously (Sakuma et al., 1994). Approximately 5×10^5 plaques were screened by plaque hybridization using the cDNA fragments of human CYP2D6 and cynomolgus monkey CYP3A8 as probes.

Expression of CYP2D21 in Yeast Cells and Analysis of Bufuralol Hydroxylase Activity. An expression plasmid for CYP2D21 was constructed with the pAAH5 yeast expression vector. The resulting expression plasmid, pAAMS2D, contains native coding, six bases of 5′-noncoding sequences, and 83 bases of 3′-noncoding sequences. Transformation of the yeast, *Saccharomyces cerevisiae* AH22, cultivation of the recombinant yeasts, preparation of microsomal fractions, and determination of P450 contents were carried out as described previously (Sakuma et al., 1994). Measurement of the bufuralol 1′-hydroxylase activity was carried out as described previously (Yokoi et al., 1996). The kinetic parameters of bufuralol 1′-hydroxylation of microsomes from the recombinant yeasts or miniature pig livers were calculated from Lineweaver-Burk plots.

Results and Discussion

To clarify the identity of the primary structure of P450 between miniature pigs and humans, two cDNA clones containing the entire coding sequence of CYP2D or CYP3A were isolated from a cDNA

TABLE 1

Comparison of the nucleotide and the deduced amino acid sequences of CYP2D6 with other CYP2D isoforms

To show genetic distance of CYP2D isoforms between human and experimental animal species, percentage of identities of respective CYP2D isoforms to human CYP2D6 were indicated. The isoforms were listed in the order of nucleotide identity to human CYP2D6. Since some isoforms have been isolated from mice, rats, guinea pigs, hamsters, and rabbits, one isoform sharing the highest identity with human CYP2D6 of each animal species was shown.

Species	Forms	Identity		Accession No.
		Nucleotide	Amino acid	
		%		
Human	2D6	100	100	M33388
Japanese monkey	2D29	97.5	95.8	AF301911
Marmoset	2D30	96.3	94.4	AY082602
Cynomolgus monkey	2D17	94.2	93.2	U38218
Marmoset	2D19	91.7	90.5	D29822
Bovine	2D14	83.8	77.5	X68481
Miniature pig	2D21	83.5	78.3	D89502
Pig	2D25	83.2	78.1	Y16417
Rabbit	2D24	82.3	78.5	AB008785
Dog	2D15	81.4	75.3	D17397
Mouse	2D22	80.1	76.1	AF221525
Rat	2D4	79.9	78.0	X52029
Hamster	2D20	77.5	73.5	D86476
Guinea pig	2D16	76.8	72.7	U21486

TABLE 2

Comparison of the nucleotide and the deduced amino acid sequences of CYP3A4 with other CYP3A isoforms

To show genetic distance of CYP3A isoforms between human and experimental animal species, percentage of identities of respective CYP3A isoforms to human CYP3A4 were indicated. The isoforms were listed in the order of nucleotide identity to human CYP3A4. Since some isoforms have been isolated from mice, rats, guinea pigs, hamsters, and dogs, one isoform sharing the highest identity with human CYP3A4 of each animal species was shown.

Species	Forms	Identity		Accession No.
		Nucleotide	Amino acid	
		%		
Human	3A4	100	100	J04449
Cynomolgus monkey	3A8	95.6	93.4	S53047
Human	3A7	94.2	88.3	D00408
Marmoset	3A21	93.5	89.5	D31921
Human	3A5	89.4	84.3	J04813
Human	3A43	84.5	75.7	AC011904
Dog	3A12	83.7	79.5	X54915
Pig	3A46	83.5	77.8	AB052266
Pig	3A29v1	82.8	76.5	Z93099
Miniature pig	3A29v5	82.5	75.3	AF424780
Pig	3A39	82.1	75.9	AF109068
Sheep	3A24	82.1	75.5	U59378
Rabbit	3A6	81.7	74.4	J05034
Miniature pig	3A22	81.5	75.0	AB006010
Bovine	3A28	81.3	73.0	Y10214
Rat	3A9	81.2	76.5	U46118
Mouse	3A13	81.2	75.5	X63023
Goat	3A19	81.2	75.2	X76530
Guinea pig	3A20	79.7	72.0	D49731
Hamster	3A31	78.2	69.2	D86951

library prepared from the liver of a male miniature pig: MS2D[2] (accession no. D89502) and MS3A (AB006010). MS2D consisted of 1613 bp including 1500 bp of an open reading frame. MS3A consisted of 1653 bp, including 1509 bp of an open reading frame. Both P450s were designated as CYP2D21 and CYP3A22 by the cytochrome P450 nomenclature committee (Nelson et al., 1996). Sequence identities of *CYP* genes of experimental animal species to human orthologous genes are summarized in Tables 1 and 2. Comparing the deduced amino acid sequences, CYP2D21 showed 78.3% identity to human CYP2D6. This value was 12.2% lower than that of the marmoset (a New World monkey) CYP2D19. CYP3A22 showed 75.0% identity to human CYP3A4. This value was 18.4% and 14.5% lower than those of the cynomolgus monkey (an Old World monkey) CYP3A8 and marmoset CYP3A21, respectively. These results indicate that miniature pig P450s are genetically not so close as monkey P450s to human P450s, although anatomical, physiological, and biochemical properties of miniature pig and human are reported to be similar.

In contrast to drug-metabolizing *CYP* genes, flavin-containing monooxygenase form 1 (M32031), dimeric dihydrodiol dehydrogenase (AB021929), and carbonyl reductase (M80709) showed 88.0, 84.4, and 84.5% amino acid sequences identities, respectively, between human and domestic pig genes. The drug-metabolizing *CYP* genes displayed relatively lower identities between human and other experimental animals except nonhuman primates than do the other drug-metabolizing enzyme genes, suggesting the presence of large species differences of function and also suggesting that these genes might not be critical to life. This might be supported by the findings that some lines of mice lacking a drug-metabolizing P450 show no abnormalities (Liang et al., 1996).

Three *CYP3A* genes from domestic pigs are found in the DNA DataBank of Japan/European Molecular Biology Laboratory/GenBank database: CYP3A29 (Z93099), CYP3A39 (AF109068), and CYP3A46 (AB052266). Those isoforms share 81.5, 83.9, and 76.5% amino acid sequence identities with CYP3A22, respectively, indicating that three domestic pig CYP3As are not an ortholog of CYP3A22.

Regarding the substrate specificity of CYP2D isoform in domestic and miniature pigs, Skaanild and Friis (1999) reported that livers of miniature pig and domestic pig have no CYP2D6 activity (debrisoquine 4-hydroxylase activity). They concluded in a later report (Skaanild and Friis, 2002) that dextromethorphan *O*-demethylase and bufuralol 1′-hydroxylase activities, other marker activities, may be catalyzed by CYP2B isoforms in domestic and miniature pigs. Low debrisoquine 4-hydroxylase activity of domestic pig CYP2D25 was confirmed by an assay using recombinant enzymes (Hosseinpour and Wikvall, 2000). By contrast, Jurima-Romet et al. (2000) demonstrated the evidence for the catalysis of dextromethorphan *O*-demethylation by a CYP2D6-like enzyme in domestic pig liver. These discrepancies raised the question of whether CYP2D enzymes of domestic or miniature pigs retain the functional similarity to human CYP2D6. Therefore, CYP2D21 was expressed in yeast cells. The recombinant CYP2D21 showed bufuralol 1′-hydroxylase activity. The apparent K_m and V_{max} values calculated from Lineweaver-Burk plots were 0.98 μM and 1.8 pmol/min/nmol P450, respectively. Those values of the human CYP2D6 expressed in the same expression system are 4.2 μM and 2.4 pmol/min/nmol P450, respectively (Yokoi et al., 1996). These results indicate that the miniature pig possesses a CYP2D enzyme in its liver, and it retains the capacity to metabolize a substrate of human CYP2D6. This, together with the finding of Skaanild and Friis (2002), implies that the contribution of CYP2D21 to the metabolism of bufuralol is smaller than those of other P450s, such as CYP2B.

The amino acid sequence of domestic pig CYP2D25 showed 97.8% identity to that of miniature pig CYP2D21. There are 10 amino acid differences between CYP2D21 and CYP2D25, and one located in the putative substrate recognition site (SRS) for CYP2 enzyme (SRS-1 through SRS-6) described by Gotoh (1992): 204th, Q or L for 2D21 or 2D25, respectively. Therefore, one could not completely exclude

[2] The P450s coded by MS2D and MS3A were designated as CYP2D21 and CYP3A22, respectively, by the cytochrome P450 nomenclature committee. The nucleotide sequences of CYP2D21 and CYP3A22 appear in the Genome Sequence DataBase, DNA DataBank of Japan, European Molecular Biology Laboratory, and National Center for Biotechnology Information databases with the accession numbers D89502 and AB006010, respectively.

the possibility that CYP2D21 and CYP2D25 have distinct substrate specificity.

Acknowledgments. We thank Dr. Frank J. Gonzalez for providing the cDNA clone of human and CYP2D6.

Laboratory of Drug Metabolism, TSUTOMU SAKUMA
Division of Pharmacobio-dynamics, TSUKASA SHIMOJIMA
Graduate School of Pharmaceutical Sciences, KIYOSHI MIWA
Hokkaido University, Sapporo, TETSUYA KAMATAKI
Japan (T.Sa., T.Sh., K.M., T.K.) and
Department of Toxicology,
Faculty of Pharmaceutical Sciences,
Toyama Medical and Pharmaceutical
University, Toyama, Japan (T.Sa.)

References

Caldwell J (1981) The current status of attempts to predict species differences in drug metabolism. *Drug Metab Rev* **12**:221–237.

Gotoh O (1992) Substrate recognition sites in cytochrome P450 family 2 (CYP2) proteins inferred from comparative analyses of amino acid and coding nucleotide sequences. *J Biol Chem* **267**:83–90.

Hosseinpour F and Wikvall K (2000) Porcine microsomal vitamin D3 25-hydroxylase (CYP2D25). Catalytic properties, tissue distribution and comparison with human CYP2D6. *J Biol Chem* **275**:34650–34655.

Jurima-Romet M, Casley WL, Leblanc CA, and Nowakowska M (2000) Evidence for the catalysis of dextromethorphan O-demethylation by a CYP2D6-like enzyme I pig liver. *Toxicol In Vitro* **14**:253–263.

Khan MA (1984) Minipig: advantages and disadvantages as a model in toxicity testing. *J Am Coll Toxicol* **3**:337–342.

Liang HCL, Li H, McKinnon RA, Duffy JJ, Potter SS, Puga A, and Nebert DW (1996) *Cyp1a2*(−/−) null mutant mice develop normally but show deficient drug metabolism. *Proc Natl Acad Sci USA* **93**:1671–1676.

Nelson DR, Koymans L, Kamataki T, Stegeman JJ, Feyereisen R, Waxman DJ, Waterman MR, Gotoh O, Coon M, Estabrook RW, et al. (1996) P450 superfamily: update on new sequences, gene mapping, accession numbers and nomenclature. *Pharmacogenetics* **6**:1–42.

Nissen PH, Wintero AK, and Fredholm M (1998) Mapping of porcine genes belonging to two different cytochrome P450 subfamilies. *Anim Genet* **29**:7–11.

Postlind H, Axen E, Bergman T, and Wikvall K (1997) Cloning, structure and expression of a cDNA encoding vitamin D3 25-hydroxylase. *Biochem Biophys Res Commun* **241**:491–497.

Sakuma T, Masaki K, Itoh S, Yokoi T, and Kamataki T (1994) Sex-related difference in the expression of cytochrome P450 in hamsters: cDNA cloning and examination for the expression of three distinct CYP2C cDNAs. *Mol Pharmacol* **45**:228–236.

Skaanild MT and Friis C (1999) Cytochrome P450 sex differences in minipigs and conventional pigs. *Pharmacol Toxicol* **85**:174–180.

Skaanild MT and Friis C (2002) Is cytochrome P450 CYP2D activity present in pig liver? *Pharmacol Toxicol* **91**:198–203.

Swindle MM and Smith AC (1998) Comparative anatomy and physiology of the pig. *Scand J Lab Anim Sci Suppl* **25**:11–22.

Watanabe FD, Mullon CJP, Hewitt WR, Arkadopoulos N, Kahaku E, Eguchi S, Khalili T, Arnaout W, Shackleton CR, Rozga J, et al. (1997) Clinical experience with a bioartificial liver in the treatment of severe liver failure A phase I clinical trial. *Ann Surg* **225**:484–491.

Yokoi T, Kosaka Y, Chida M, Chiba K, Nakamura H, Ishizaki T, Kinoshita M, Sato K, Gonzalez FJ, and Kamataki T (1996) A new CYP2D6 allele with a nine base insertion in exon 9 in a Japanese population associated with poor metabolizer phenotype. *Pharmacogenetics* **6**:395–401.

Zaphiropoulos PG, Skantz A, Eliasson M, and Ahlberg MB (1995) Cytochrome P450 genes expressed in porcine ovaries: identification of novel forms, evidence for gene conversion and evolutionary relationships. *Biochem Biophys Res Commun* **212**:433–441.

Drug Metab. Pharmacokin. 19 (2): 120-129 (2004).

Regular Article

CYP3A5 Contributes Significantly to CYP3A-mediated Drug Oxidations in Liver Microsomes from Japanese Subjects

Satoshi YAMAORI[1], Hiroshi YAMAZAKI[1], Shunsuke IWANO[1], Kazuma KIYOTANI[1], Keiko MATSUMURA[1], Goro HONDA[2], Kazuko NAKAGAWA[3], Takashi ISHIZAKI[3] and Tetsuya KAMATAKI[1]

[1]*Laboratory of Drug Metabolism, Graduate School of Pharmaceutical Sciences, Hokkaido University, Sapporo, Japan*
[2]*Saiseikai Kumamoto Hospital, Kumamoto, Japan*
[3]*Department of Pharmacology and Therapeutics, Graduate School of Clinical Pharmacy, Kumamoto University, Kumamoto, Japan*

Full text of this paper is available at http://www.jssx.org

Summary: The purpose of this study was to evaluate a contribution of polymorphic cytochrome P450 (CYP) 3A5 to the oxidation of diltiazem, midazolam and testosterone by liver microsomes from Japanese subjects. Twenty-seven liver samples were classified into three groups according to the *CYP3A5* genotypes; *CYP3A5*1/*1* (n=3), **1/*3* (n=12) and **3/*3* (n=12). The results of genotyping and immunochemical quantitation of CYP3A5 protein showed a good accordance between the *CYP3A5* genotype and CYP3A5 content but not CYP3A4 content in liver microsomes. The expression levels of hepatic CYP3A5 protein ranged from 20 to 60% of the sum of CYP3A4 and CYP3A5 contents in subjects with at least one wild type allele (**1*). The CYP3A5 contents correlated well with liver microsomal activities of diltiazem *N*-demethylation, midazolam 1′- and 4-hydroxylations and testosterone 6β-hydroxylation among subjects carrying at least one **1* allele. In addition, the correlation coefficients of CYP3A5 contents with the rates of diltiazem *N*-demethylation, midazolam 1′-hydroxylation and testosterone 6β-hydroxylation were higher than those of CYP3A4, although the value of CYP3A5 with the midazolam 4-hydroxylation rate was similar to that of CYP3A4. Kinetic analyses revealed a biphasic diltiazem *N*-demethylation in liver microsomes from subjects carrying the **1* allele. The apparent V_{max}/K_m values for recombinant CYP3A5 indicated the greater contributions to diltiazem *N*-demethylation and midazolam 1′-hydroxylation as compared with CYP3A4. These results suggest that polymorphic CYP3A5 contributes markedly to the drug oxidations, particularly diltiazem *N*-demethylation, midazolam 1′-hydroxylation and testosterone 6β-hydroxylation by liver microsomes from Japanese subjects.

Key words: CYP3A5; polymorphism; liver; diltiazem; midazolam; testosterone

Introduction

Cytochrome P450 (CYP) comprises a superfamily of enzymes responsible for the oxidations of various endogenous and exogenous compounds including drugs, toxicants and procarcinogens.[1)] CYP3A is one of the major subfamilies of CYP expressed in human livers.[2)] This subfamily has been known to be involved in the metabolism of more than 50% of clinically used drugs,

This work was supported in part by a Grant-in-Aid (No. 99-2) from the Organization for Pharmaceutical Safety and Research (OPSR) and Ministry of Education, Science, Sports and Culture of Japan. This work was also supported in part by a Grant-in-Aid from the Ministry of Health, Labour and Welfare of Japan, a Grant-in-Aid from the Core Research for Evolutional Science and Technology, and an SRF Grant for Biomedical Research in Japan.

Received; November 12, 2003, Accepted; January 8, 2004
To whom correspondence should be addressed: Satoshi YAMAORI, *Department of Hygienic Chemistry, Faculty of Pharmaceutical Sciences, Hokuriku University, 3-Ho, Kanagawa-machi, Kanazawa 920-1181, Japan. Tel. +81-76-229-1165 (342), Fax. +81-76-229-6221, E-mail: s-yamaori@hokuriku-u.ac.jp*
Send reprint requests to: Tetsuya KAMATAKI, Ph.D. Laboratory of Drug Metabolism, Graduate School of Pharmaceutical Sciences, Hokkaido University, N12W6, Kita-ku, Sapporo 060-0812, Japan. Tel. +81-11-706-3233, Fax. +81-11-706-4978, E-mail: kamataki@pharm.hokudai.ac.jp

such as diltiazem, midazolam and erythromycin.[3] CYP3As are also responsible for the bioactivation of procarcinogens including aflatoxin B_1.[4,5]

The human CYP3A subfamily consists of CYP3A4,[6,7] CYP3A5,[8-10] CYP3A7[11] and CYP3A43.[12] CYP3A4 is the most abundant form of CYP3A (~30% of the total CYP content) expressed in human adult livers.[2] CYP3A7 was originally isolated from human fetal livers[11] and was demonstrated as a fetal-specific form of CYP3A,[13] while a few reports have appeared on the existence of CYP3A7 in adult livers from normal Caucasian subjects[14] and Japanese patients with hepatocellular carcinoma.[15] CYP3A43 is a minor isoform of CYP3A expressed in adult livers.[12] CYP3A5 is polymorphically expressed in human adult and fetal livers.[8,9] Recently, it was demonstrated that the polymorphic expression of CYP3A5 is mainly attributed to a single nucleotide substitution in intron 3, referred to as *CYP3A5*3*.[16] The content of CYP3A5 accounts for approximately 20% of CYP3A contents in adult livers.[9] A recent report has also shown that CYP3A5 is expressed at an equivalent level of CYP3A4 in some livers of Caucasians and African Americans.[16]

CYP3A5 is capable of catalyzing midazolam 1′-hydroxylation more efficiently than CYP3A4.[17] It has also been reported that CYP3A5 expressed in liver microsomes from Caucasians and African Americans contributes to midazolam metabolism.[16] However, the contribution of CYP3A5 to the other CYP3A-mediated drug oxidations has not been examined extensively.

The purpose of this study was to clarify the role of CYP3A5 in the drug oxidations in liver microsomes from Japanese subjects. We report herein that CYP3A5 contributes to the metabolism of diltiazem, midazolam and testosterone to different extents. In particular, CYP3A5 exhibited great contributions to the diltiazem *N*-demethylation, midazolam 1′-hydroxylation and testosterone 6β-hydroxylation, whereas CYP3A5 and CYP3A4 contributed equally to the midazolam 4-hydroxylation.

Materials and Methods

Materials: *N*-Desmethyldiltiazem was a gift from Tanabe Seiyaku (Osaka, Japan). Rabbit anti-human CYP3A4 antibodies were provided by Nosan Corporation (Tokyo, Japan). Rabbit anti-human CYP3A5 antibodies were purchased from Gentest (Woburn, MA). Other chemicals were obtained from the following sources: midazolam, 1′- and 4-hydroxymidazolam and 6β-hydroxytestosterone were from Daiichi Pure Chemicals (Tokyo, Japan); diltiazem and testosterone were from Wako Pure Chemicals (Osaka, Japan); $NADP^+$, glucose 6-phosphate and glucose 6-phosphate dehydrogenase were from Oriental Yeast (Tokyo, Japan). All other chemicals were of the highest grade commercially available.

Human liver microsomes: Human livers were obtained from patients after pathological examination of specimens isolated after death or during hepatic surgery.[18] The use of the human livers for these studies was approved by the Ethics Committee of Hokkaido University. Liver samples were stored at −80°C until use. Liver microsomes were prepared and suspended in 10 mM Tris-HCl buffer (pH 7.4) containing 1 mM EDTA and 20% (v/v) glycerol as described previously.[19] The microsomal protein was determined by using Pierce BCA Protein Assay Kit (Pierce Chemical, Rockford, IL) with bovine serum albumin as a standard.

Genotyping of genomic DNA from human livers: Genomic DNA was isolated from human livers according to a method reported previously.[20] A genotyping method for the mutated allele (**3*) of the *CYP3A5* gene was performed using a real-time polymerase chain reaction (PCR) and fluorescent probe melting point analysis on the LightCycler™ (Roche Diagnostics, Somerville, NJ). Oligonucleotide primers were designed using the *CYP3A5* sequence obtained from GenBank database (accession number; NT_031809.1). A 318-bp fragment of the intron 3 of the *CYP3A5* gene was amplified using the primers 3A5*3F (5′-CTT AAC GAA TGC TCT ACT GTC-3′) and 3A5*3R (5′-AGT TGA CCT TCA TAC GTT CTG-3′). The mutation site in the *CYP3A5*3* allele was covered by a mutant detection probe LC3A5*3-FITC (5′-TGT CTT TCA GTA TCT CTT C-3′) which was labeled with fluorescein at the 3′-terminus. The adjacent anchor probe LC3A5*3-Red640 (5′-CTG TTT GGA CCA CAT TAC CC-3′) was labeled with the LightCycler Red640 at the 5′-terminus and phosphorylated at the 3′-terminus. PCR reactions were carried out in a final volume of 20 μL consisting of 50 ng of genomic DNA, 3.0 mM $MgCl_2$, 0.5 μM amplification primers 3A5*3F and 3A5*3R, 0.2 μM LC3A5*3-FITC probe and 0.4 μM LC3A5*3-Red640 anchor. As a reaction buffer, the LightCycler FastStart DNA Master Hybridization Probes were used (Roche Molecular Biochemicals, Mannheim, Germany). The cycling program consisted of a 10 min initial denaturation at 95°C and 50 cycles of 95°C for 5 s, 60°C for 5 s and 72°C for 12 s, with a maximum ramp rate. The analytical melting program was 95°C for 30 s and 40°C for 30 s, increasing to 65°C at a ramp rate of 0.1°C/s, with continuous fluorescence acquisition.

Immunoquantitation of CYP3A5 and CYP3A4 proteins expressed in human liver microsomes: SDS-PAGE was performed using an 8% acrylamide gel as described previously.[21] Microsomal protein (5–10 μg) was separated and transferred onto an Immobilon membrane (Millipore, Bedford, MA). Immunoblot quantitation was performed using rabbit antibodies to human CYP3A5 and CYP3A4 as primary antibodies and

horseradish peroxidase-conjugated anti-rabbit immunoglobulin (Gentest) as a secondary antibody. CYP3A5 and CYP3A4 proteins were visualized by staining with 3′-diaminobenzidine. Expression levels of these proteins were quantified from calibration curves obtained with microsomal protein from baculovirus-infected insect cells expressing recombinant human CYP3A5 and CYP3A4 (Gentest), respectively.

Preparation of membrane fraction from genetically engineered *E. coli* cells expressing CYP3A5 or CYP3A4 and NADPH-cytochrome P450 reductase: The 5′-terminus of CYP3A5 cDNA was modified as described previously.[22] A bicistronic plasmid carrying CYP3A5 and the NADPH-cytochrome P450 reductase (reductase) cDNAs was constructed according to the method reported by Iwata *et al.*[23] *E. coli* DH5α strain harboring CYP3A4 together with the reductase was established by Iwata *et al.*[23] CYP3A5 or CYP3A4 and the reductase in the genetically engineered *E. coli* cells were expressed as reported previously.[23] Membranes were prepared from *E. coli* cells harboring each isoform of CYP3A and the reductase as described previously.[24] The fraction was suspended in 100 mM Tris-HCl buffer (pH 7.5) containing 20% (v/v) glycerol and stored at −80°C until use. The content of CYP in the membrane fraction was determined according to the method reported previously.[25] The reductase activity was measured as described previously.[26] One unit of the reductase was defined as the amount of the enzyme that reduced 1 μmol of cytochrome *c*/min. Human cytochrome b_5 (b_5) in the genetically engineered *E. coli* cells was expressed following a method of Holmans *et al.*[27] and purified as reported previously.[28]

Enzyme assays: Unless otherwise stated, a typical incubation mixture consisted of 100 mM sodium potassium phosphate buffer (pH 7.4), 50 μM EDTA, a substrate and human liver microsomes (75 μg protein) in a final volume of 200 μL. After preincubation at 37°C for 5 min, reactions were initiated by the addition of an NADPH-generating system (0.5 mM $NADP^+$, 5 mM glucose 6-phosphate and 1 unit/mL glucose 6-phosphate dehydrogenase). All determinations were performed in duplicate.

Diltiazem *N*-demethylase activity was determined as described below. An incubation mixture consisted of 5 to 500 μM diltiazem. Incubations were carried out at 37°C for 10 min and terminated by adding 10 μL of 70% (w/v) perchloric acid. After removal of protein by centrifugation, 150 μL of the supernatant was subjected to high-performance liquid chromatography equipped with a Mightysil RP-18 GP column (4.6×150 mm, 5 μm, Kanto Chemical, Tokyo, Japan). Fifty mM potassium phosphate buffer (pH 6.0) containing 30% (v/v) acetonitrile was used as a mobile phase. Elution was performed at a flow rate of 1.5 mL/min. The formation of *N*-desmethyldiltiazem was monitored at a wavelength of 238 nm.

Midazolam 1′- and 4-hydroxylase activities were determined as described previously,[29] except that an incubation mixture contained 100 mM potassium phosphate buffer (pH 7.4) and 10 μM midazolam. Incubations were carried out at 37°C for 10 min and terminated by adding 200 μL of cold methanol. After removal of protein by centrifugation, 200 μL of the supernatant was subjected to high-performance liquid chromatography equipped with a Mightysil RP-18 GP column (4.6×150 mm, 5 μm, Kanto Chemical).

Testosterone 6β-hydroxylase activity was determined according to the method reported previously,[30] except that the typical incubation mixture contained 50 μM testosterone in a final volume of 250 μL.

Kinetic analyses of oxidations catalyzed by CYP3A expressed in *E. coli* membranes: Membranes from *E. coli* cells coexpressing CYP3A5 or CYP3A4 and the reductase, and a purified recombinant human b_5 preparation were employed as the enzyme source. Incubations were performed as described in the enzyme assays, except that incubation mixtures consisted of 10 pmol of CYP3A and 20 pmol of b_5 (for the *N*-demethylation of diltiazem) or 5 pmol of CYP3A and 10 pmol of b_5 (for the 1′- and 4-hydroxylations of midazolam and 6β-hydroxylation of testosterone). To determine kinetic parameters, substrate concentrations ranged from 0.78 to 400 μM (diltiazem), from 0.78 to 100 μM (midazolam) and from 12.5 to 500 μM (testosterone). Data points were fitted to the Michaelis-Menten equation by nonlinear least-squares regression analysis with Origin 6.1J software (OriginLab, Northampton, MA).

Statistical analyses: Univariate or multivariate linear regression analysis was performed to compare oxidation rates with contents of CYP3A4 and/or CYP3A5 using a program InStat (GraphPad Software, San Diego, CA). Analysis of variance was used to determine whether the model was statistically significant with $p<0.05$.

Results

Genotyping of the *CYP3A5* gene: We developed a rapid and a reproducible genotyping method for the wild type allele (**1*) and mutated allele (**3*) using a real-time PCR. Melting curves after PCR reactions for the *CYP3A5*1/*1*, **1/*3* and **3/*3* genotypes are shown in **Fig. 1**. Individuals with the *CYP3A5*1/*1* genotype had the lowest melting temperature (Tm) at 48°C. Individuals with the *CYP3A5*1/*3* genotype had two Tms at 48°C and 55°C. Individuals with the *CYP3A5*3/*3* genotype had the highest Tm at 55°C. Accordingly, liver samples from 27 Japanese subjects were genotyped for the *CYP3A5*1/*1* (n=3), **1/*3* (n=12) and **3/*3* (n=12).

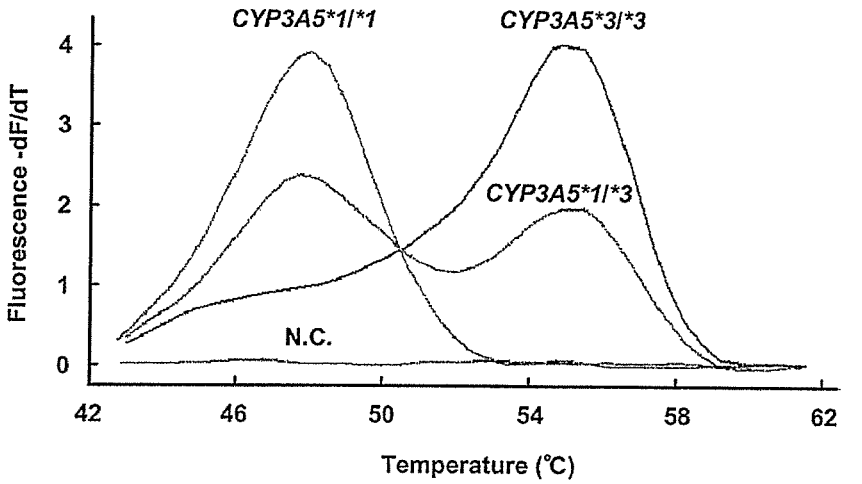

Fig. 1. Melting peak patterns for the *CYP3A5*1/*1*, **1/*3* and **3/*3* genotypes. The melting curves were obtained after 50 cycles of real-time PCR with the primers specific for the intron 3 of the *CYP3A5* gene. The peaks of the negative first derivative of fluorescence with respect to temperature (-dF/dT) represent Tm. An individual with the *CYP3A5*1/*1* genotype has the lowest Tm at 48°C. An individual with the *CYP3A5*1/*3* genotype has two Tms at 48°C and 55°C. An individual with the *CYP3A5*3/*3* genotype has the highest Tm at 55°C. N.C. is the negative control.

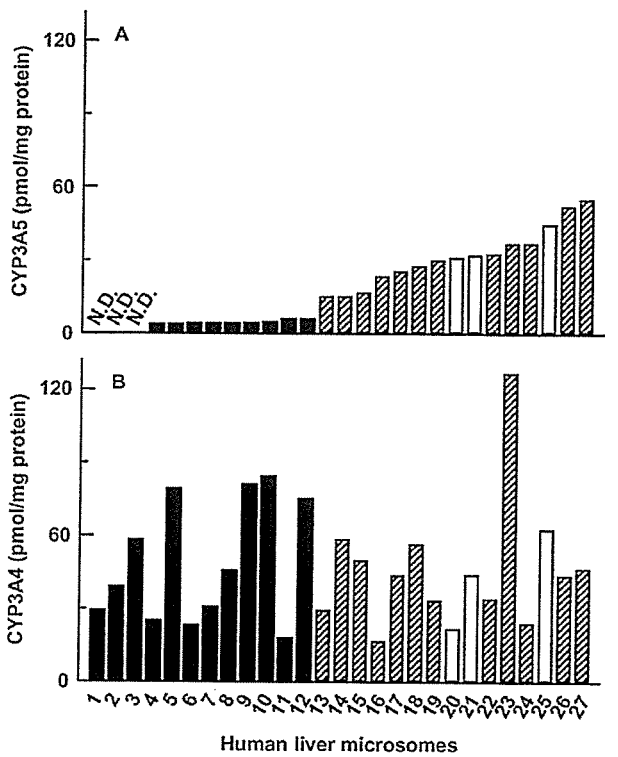

Fig. 2. Relationship between the expression levels of CYP3A5 (A) or CYP3A4 (B) proteins in liver microsomes and the *CYP3A5* genotypes of Japanese subjects. Liver microsomes (5–10 μg protein) were applied to immunoblotting analyses. Open, hatched and closed columns represent the subjects with the *CYP3A5*1/*1*, **1/*3* and **3/*3* genotypes, respectively. Samples were ranked according to the contents of CYP3A5 protein. N.D., not detectable (<1.0 pmol/mg protein).

Association of CYP3A5 and CYP3A4 contents with the *CYP3A5* genotypes: The expression levels of CYP3A5 and CYP3A4 proteins were determined immunochemically with liver microsomes from the 27 Japanese subjects (**Fig. 2**). Liver microsomes from subjects with the *CYP3A5*1/*1* or **1/*3* genotypes expressed CYP3A5 protein ranging from 15 to 55 pmol/mg protein, accounting for 20 to 60% of the sum of CYP3A4 and CYP3A5 contents (**Fig. 2A**). On the other hand, the expression level of CYP3A5 in liver microsomes of subjects homozygous for the mutated allele (**3*) was less than 5 pmol/mg protein (**Fig. 2A**). CYP3A4 was expressed in all liver samples examined; the content varied from 17 to 127 pmol/mg protein (**Fig. 2B**). There was no difference in the mean expression level of CYP3A4 between subjects possessing the *CYP3A5*1/*1* or **1/*3* genotypes and the *CYP3A5*3/*3* genotype (46±26 and 49±25 pmol/mg protein, mean±S.D., respectively), indicating that the mutated allele (**3*) of the *CYP3A5* gene does not affect the expression level of CYP3A4. Total CYP3A content in liver microsomes from subjects with at least one wild type allele (**1*) (78±31 pmol/mg protein, n=15) was significantly higher than that from subjects with the *CYP3A5*3/*3* genotype (53±26 pmol/mg protein, n=12, $p=0.03$).

Correlation between catalytic activities and CYP3A contents in individual liver microsomes from Japanese subjects: To clarify the involvement of CYP3A5 in the diltiazem *N*-demethylation, we examined a correlation between the activities and CYP3A5 or CYP3A4 contents in individual liver microsomes from subjects with different *CYP3A5* genotypes (**Fig. 3**). The sum of

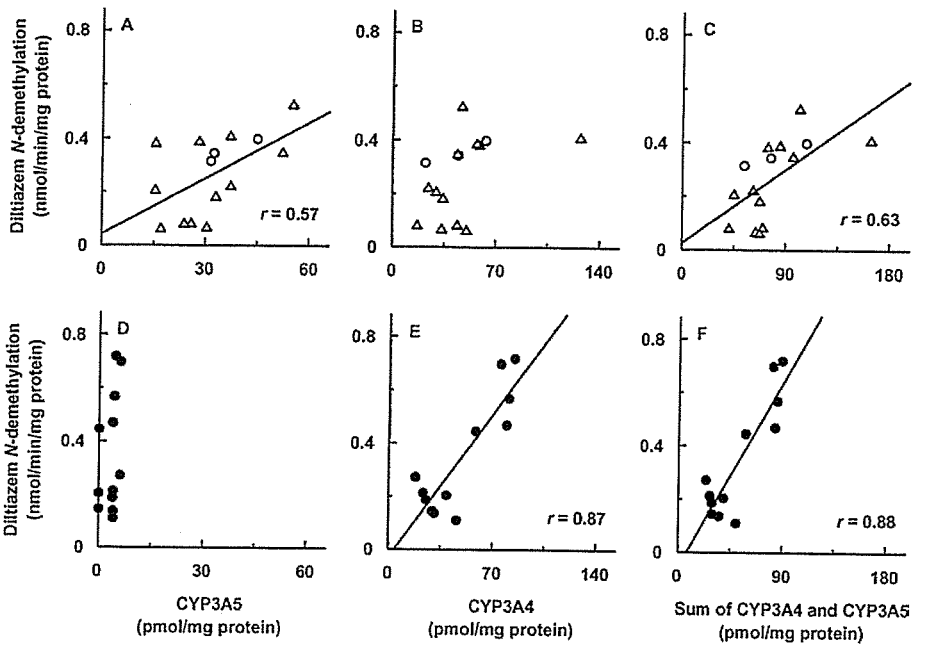

Fig. 3. Correlation between diltiazem *N*-demethylase activities and CYP3A contents in individual liver microsomes of subjects with the *CYP3A5*1/*1* or **1/*3* (A-C) and *CYP3A5*3/*3* (D-F) genotypes. Rates of the diltiazem *N*-demethylation at a substrate concentration of 20 μM were determined with liver microsomes from subjects carrying the *CYP3A5*1/*1* (○), **1/*3* (△) and **3/*3* (●) genotypes as described in the text. The univariate linear regression analysis was performed to compare the *N*-demethylase activities with the contents of CYP3A5, CYP3A4 and sum of these CYP3A proteins. Respective correlation coefficients represent statistically significant linear regression of the *N*-demethylase activities and CYP3A contents with $p<0.05$.

Table 1. Correlation between drug oxidation rates and CYP3A contents in individual liver microsomes from subjects with different *CYP3A5* genotypes

Reaction	Substrate concn. (μM)	Correlation coefficient, R^{2a}				
		*CYP3A5*1/1* or **1/*3* (n=15)			*CYP3A5*3/*3* (n=12)	
		CYP3A5	CYP3A4	CYP3A4+3A5	CYP3A4	CYP3A4+3A5
Diltiazem *N*-demethylation	20	0.32[b]	0.22	0.47[b,d]	0.76[c]	0.79[c,i]
	200	0.42[c]	0.34[b]	0.65[c,e]	0.77[c]	0.79[c,i]
Midazolam 1′-hydroxylation	10	0.38[b]	0.21	0.51[b,f]	0.74[c]	0.77[c,i]
Testosterone 6β-hydroxylation	50	0.33[b]	0.24	0.50[b,g]	0.76[c]	0.78[c,i]
Midazolam 4-hydroxylation	10	0.32[b]	0.30[b]	0.53[b,h]	0.78[c]	0.78[c,i]

[a]Determined by the univariate (CYP3A5 or CYP3A4 contents) or multivariate (CYP3A4+3A5 contents) linear regression.
[b]Statistically significant in the linear regression of the oxidation activities and CYP3A contents with $p<0.05$.
[c]Statistically significant in the linear regression of the oxidation activities and CYP3A contents with $p<0.01$.
[d]The amounts of CYP3A5 but not CYP3A4 made a significant contribution with $p<0.05$ and $p=0.10$, respectively.
[e]The CYP3A5 and CYP3A4 contents made a significant contribution with $p<0.01$ and $p<0.05$, respectively.
[f]The amounts of CYP3A5 but not CYP3A4 made a significant contribution with $p<0.05$ and $p=0.09$, respectively.
[g]The amounts of CYP3A5 but not CYP3A4 made a significant contribution with $p<0.05$ and $p=0.07$, respectively.
[h]The CYP3A5 and CYP3A4 contents made a significant contribution with $p<0.05$.
[i]The amounts of CYP3A4 but not CYP3A5 made significant contributions with $p<0.01$ and $p>0.24$, respectively.

CYP3A4 and CYP3A5 contents in liver samples of subjects carrying at least one wild type allele (**1*) correlated well with the *N*-demethylase activities (**Fig. 3C**). Furthermore, the CYP3A5 contents showed a fairly good correlation with the activities in contrast to CYP3A4 contents (**Figs. 3A** and **3B**), suggesting that CYP3A5 is responsible for the *N*-demethylation. On the other hand, the CYP3A4 contents and sum of CYP3A4 and CYP3A5 contents correlated highly with the activities of liver microsomes from subjects homozygous for the mutated allele (**3*) (**Figs. 3E** and **3F**).

Correlation coefficients between CYP3A5 and/or

CYP3A4 contents and the drug oxidation rates in individual liver microsomes are summarized in **Table 1**. Good correlations of CYP3A5 contents with all the oxidations examined were seen in liver microsomes from subjects carrying the *CYP3A5*1/*1* or **1/*3* genotypes. In contrast, the CYP3A4 contents correlated only with the diltiazem *N*-demethylation at a substrate concentration of 200 μM and midazolam 4-hydroxylation. Multivariate regression analyses showed that the amounts of CYP3A4 plus CYP3A5 correlated significantly with all the oxidation rates studied in liver microsomes from subjects with at least one wild type allele (**1*) ($0.47 \leq R^2 \leq 0.65$, $p < 0.05$). There were significant contributions of the CYP3A5 contents to all the oxidations examined ($p < 0.05$), although CYP3A4 contents significantly contributed only to the diltiazem *N*-demethylation at a substrate concentration of 200 μM and midazolam 4-hydroxylation ($p < 0.05$). The correlation coefficients of CYP3A5 contents with the rates of diltiazem *N*-demethylation, midazolam 1′-hydroxylation and testosterone 6β-hydroxylation were greater as compared with those of CYP3A4, suggesting that CYP3A5 may contribute markedly to these oxidations. In the midazolam 4-hydroxylation, the coefficient with CYP3A5 contents was similar to that with CYP3A4 contents. In liver microsomes from the subjects with the *CYP3A5*3/*3* genotype, on the other hand, the CYP3A4 contents and CYP3A4 plus CYP3A5 contents correlated highly with all the drug oxidation rates investigated ($p < 0.01$). Correlation coefficients of CYP3A4 contents with the activities were comparable to those of CYP3A4 plus CYP3A5 contents, indicating that CYP3A4 may contribute largely to the oxidations in liver microsomes with little or no expression of CYP3A5. Lower correlation coefficients between CYP3A4 contents and the drug oxidation rates were seen in liver samples of subjects carrying at least one wild type allele (**1*) in comparison to those of subjects with the *CYP3A5*3/*3* genotype, being considered that the polymorphic expression of CYP3A5 led to relatively minor contributions of CYP3A4 to the oxidations.

Role of CYP3A5 in diltiazem *N*-demethylation: Eadie-Hofstee plots for the diltiazem *N*-demethylation by liver microsomes from subjects homozygous for the wild type allele (**1*) or mutated allele (**3*) are shown in **Fig. 4**. A biphasic pattern in the *N*-demethylation was seen in the liver microsomes from a subject carrying the *CYP3A5*1/*1* genotype, although those from a subject with the *CYP3A5*3/*3* genotype showed a monophasic pattern, suggesting that not only CYP3A4 but also CYP3A5 are involved in the oxidation by liver microsomes from the subject with the *CYP3A5*1* allele.

Examination for the relative contributions of CYP3A5 and CYP3A4 to drug oxidations using the membrane fraction of genetically engineered *E. coli*: To support an assumption on the relative contributions of CYP3A5 and CYP3A4 to the metabolism of diltiazem, midazolam and testosterone, kinetic parameters for the oxidations were determined by using CYP3A5 and CYP3A4 expressed in *E. coli* membranes (**Table 2**). In diltiazem *N*-demethylation and midazolam 1′-hydro-

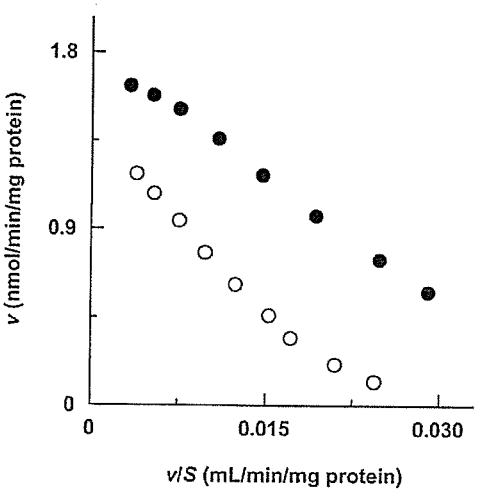

Fig. 4. Representative Eadie-Hofstee plots for the *N*-demethylation of diltiazem by liver microsomes with the *CYP3A5*1/*1* (○) and **3/*3* (●) genotypes.

Table 2. Drug oxidations catalyzed by CYP3A5 and CYP3A4 expressed in *E. coli* membranes.

Reaction	CYP	K_m (μM)	V_{max} (nmol/min/nmol CYP3A)	V_{max}/K_m (mL/min/nmol CYP3A)
Diltiazem *N*-demethylation	3A5	190 ± 6	30 ± 1	0.16 ±0.01
	3A4	110 ±10	7.2± 0.3	0.065±0.007
Midazolam 1′-hydroxylation	3A5	5.9± 0.8	20 ± 1	3.4 ±0.5
	3A4	7.0± 0.9	10 ± 1	1.4 ±0.1
Testosterone 6β-hydroxylation	3A5	400 ±80	180 ±15	0.45 ±0.07
	3A4	110 ±16	120 ± 7	1.1 ±0.2
Midazolam 4-hydroxylation	3A5	50 ±16	2.6± 0.4	0.052±0.019
	3A4	21 ± 5	6.1± 0.4	0.29 ±0.07

Values are mean±S.E. of kinetic parameters.

xylation, the apparent V_{max}/K_m values for CYP3A5 were 2.5 and 2.4 times higher than those for CYP3A4, respectively, supporting the surmise that CYP3A5 contributes markedly to these oxidations in liver microsomes from subjects with at least one wild type allele (**1*). On the other hand, the values for the testosterone 6β-hydroxylation and midazolam 4-hydroxylation by CYP3A5 were 0.41 and 0.18 of those for CYP3A4, respectively.

Discussion

Polymorphism of the *CYP3A5* gene can be mainly explained by the *CYP3A5*3* and **6* alleles, which cause alternative splicing and protein truncation.[16] However, a recent report has shown that 200 healthy Japanese subjects carry the *CYP3A5*1* and/or **3* alleles but not *CYP3A5*6* allele.[31] Thus, we developed a rapid genotyping method allowing us to distinguish the wild type (**1*) and mutated (**3*) alleles using a real-time PCR. The allelic frequency of the wild type allele (**1*) in Japanese was 33%. This value is similar to that reported previously by Hustert *et al.*,[32] but is greater than that reported by Fukuen *et al.*[31] The frequencies of the *CYP3A5*1/*1* and **1/*3* genotypes in this study were estimated as 11.1 and 44.4%, respectively, which were higher than those reported by Fukuen *et al.*[31]

A good relationship between the *CYP3A5* genotype and expression level of CYP3A5 protein was seen in Japanese livers in the present study. CYP3A4 contents did not correlate with any of the *CYP3A5* genotypes and CYP3A5 contents, suggesting that the expression of CYP3A5 and CYP3A4 is regulated independently. This was in contrast to results that expression levels of CYP3A5 and CYP3A4 were highly correlated in the Caucasian livers with the *CYP3A5*1/*3* genotype.[33] Thus, we propose that the polymorphism of the *CYP3A5* gene does not appear to affect the expression of CYP3A4.

The expression levels of hepatic CYP3A5 protein among subjects carrying the *CYP3A5*1/*1* or **1/*3* genotypes indicate that CYP3A5 contents are higher and more variable than that reported previously.[15] It was shown that the content of CYP3A5 accounted for approximately 20% of the total CYP3A content in the liver expressing this protein.[9] However, it has been also reported that CYP3A5 represents at least 50% of the total CYP3A content in adult livers including one-third of Caucasians and more than one-half of African Americans.[16] Taken together with our results and their findings, CYP3A5 is likely to contribute markedly to the total CYP3A content not only in Caucasians and African Americans but also Japanese with at least one wild type allele (**1*).

It was demonstrated that CYP3As were major enzymes catalyzing the *N*-demethylation of diltiazem.[34] In the present study, liver microsomal activities of the *N*-demethylation correlated highly with rates of the midazolam 1′- and 4-hydroxylations and testosterone 6β-hydroxylation among subjects carrying the *CYP3A5*1/*1* and **1/*3* genotypes ($r=0.97$, 0.91 and 0.95, respectively, $p<0.01$, data not shown). In addition, the rates of the *N*-demethylation were well associated with the expression levels of hepatic CYP3A5 protein. Interestingly, liver microsomes from subjects with the wild type allele (**1*) revealed a biphasic pattern for the *N*-demethylation. These results strongly suggest that both CYP3A5 and CYP3A4 are responsible for the diltiazem *N*-demethylation. Kinetic analyses with membrane fractions prepared from genetically engineered *E. coli* cells expressing recombinant CYP3A5 and CYP3A4 showed that CYP3A5 was capable of catalyzing the *N*-demethylation more efficiently than CYP3A4, being consistent with the findings reported by Jones *et al.*[35] This supports the result that CYP3A5 contributed significantly to the *N*-demethylation in liver microsomes of subjects with at least one wild type allele (**1*).

CYP3A5 and CYP3A4 metabolize midazolam to produce two metabolites; 1′-hydroxymidazolam and 4-hydroxymidazolam. The ratio of 1′-hydroxymidazolam to 4-hydroxymidazolam depends on CYP3A isoforms and substrate concentrations.[17] A recent report by Williams *et al.*[36] has shown that the ratio for recombinant CYP3A5 is higher than that for CYP3A4 at substrate concentrations up to 100 μM. In our current study, the average ratio for the liver microsomes from subjects carrying at least one wild type allele (**1*) were higher than that for subjects with the *CYP3A5*3/*3* genotype (data not shown). This is compatible with those reported previously,[16,17] indicating that the polymorphic expression of CYP3A5 affects the metabolite ratio for the midazolam hydroxylations.

A previous report showed that CYP3A5 contents correlated well with the rates of nifedipine oxidation as estimated from the contents of each CYP3A isoform and the oxidation rates in human liver microsomes.[15] More recently, it has been reported that CYP3A5 content accounts for 32% of the variability in total midazolam hydroxylation rates (sum of formation rates of 1′- and 4-hydroxymidazolam).[33] In this study, good correlations between CYP3A5 contents and the activities of diltiazem *N*-demethylation, midazolam 1′- and 4-hydroxylations and testosterone 6β-hydroxylation were seen in liver microsomes from subjects with the *CYP3A5*1/*1* or **1/*3* genotypes. In contrast to our observation, Westlind-Johnsson *et al.*[37] failed to demonstrate that CYP3A5 contributed to the testosterone 6β-hydroxylation in liver microsomes from Caucasians. The reason for this discrepancy may be caused by a small number of liver samples expressing CYP3A5 (only $n=5$). The apparent V_{max}/K_m values for recom-

binant CYP3A5 indicated the lower contributions of this enzyme to the testosterone 6β-hydroxylation and midazolam 4-hydroxylation. These results suggest that both relative activities and amounts of CYP3A5 and CYP3A4 may determine the contribution of these CYP3A isoforms to the drug oxidations in human liver microsomes.

The question of whether CYP3A5 plays a role in the metabolism of CYP3A substrates *in vivo* is raised from our results and previous findings.[16,17] However, the effects of the *CYP3A5* genotypes on the disposition of CYP3A substrates have not been investigated extensively. A more recent study has shown that the disposition of midazolam *in vivo* was not affected by the *CYP3A5* genotypes.[38] The reason for this is yet unclear, but the role of CYP3A5 in the CYP3A-mediated drug metabolism needs to be examined as Shih and Huang[38] have pointed out. One approach is to compare the ratio of formation rates of two metabolites, such as midazolam and alprazolam, for the various *CYP3A5* genotypes, since CYP3A5 and CYP3A4 exhibit different ratios depending on the substrates used.[17,36]

CYP3A5 is a major form of CYP3A expressed in various extrahepatic tissues such as adult kidney,[39] peripheral blood,[40] normal lung and lung tumors.[41] It has been reported that CYP3A5 and CYP3A4 efficiently catalyze the 4-hydroxylation of cyclophosphamide and ifosfamide to produce therapeutically active metabolites.[42] These findings suggest the importance of CYP3A5 on the drug metabolism in these extrahepatic tissues.

In conclusion, this is the first study to demonstrate that CYP3A5 contributes to the CYP3A-mediated drug oxidations by human liver microsomes. CYP3A5 indicated a large degree of contributions to the diltiazem *N*-demethylation, midazolam 1′-hydroxylation and testosterone 6β-hydroxylation, although CYP3A5 and CYP3A4 contributed equally to the midazolam 4-hydroxylation. The present results strongly suggest that polymorphic expression of CYP3A5 may partly account for the variation in the metabolism of CYP3A substrates.

Acknowledgments: We thank Tanabe Seiyaku for providing *N*-desmethyldiltiazem and Nosan Corporation for providing rabbit anti-human CYP3A4 antibodies.

References

1) Nelson, D. R., Koymans, L., Kamataki, T., Stegeman, J. J., Feyereisen, R., Waxman, D. J., Waterman, M. R., Gotoh, O., Coon, M. J., Estabrook, R. W., Gunsalus, I. C. and Nebert, D. W.: P450 superfamily: update on new sequences, gene mapping, accession numbers and nomenclature. *Pharmacogenetics*, **6**: 1-42 (1996).
2) Shimada, T., Yamazaki, H., Mimura, M., Inui, Y. and Guengerich, F. P.: Interindividual variations in human liver cytochrome P-450 enzymes involved in the oxidation of drugs, carcinogens and toxic chemicals: studies with liver microsomes of 30 Japanese and 30 Caucasians. *J. Pharmacol. Exp. Ther.*, **270**: 414-423 (1994).
3) Rendic, S.: Summary of information on human CYP enzymes: human P450 metabolism data. *Drug Metab. Rev.*, **34**: 83-448 (2002).
4) Kitada, M., Taneda, M., Ohi, H., Komori, M., Itahashi, K., Nagao, M. and Kamataki, T.: Mutagenic activation of aflatoxin B_1 by P-450 HFLa in human fetal livers. *Mutat. Res.*, **227**: 53-58 (1989).
5) Shimada, T. and Guengerich, F. P.: Evidence for cytochrome $P\text{-}450_{NF}$, the nifedipine oxidase, being the principal enzyme involved in the bioactivation of aflatoxins in human liver. *Proc. Natl. Acad. Sci. USA*, **86**: 462-465 (1989).
6) Beaune, P. H., Umbenhauer, D. R., Bork, R. W., Lloyd, R. S. and Guengerich, F. P.: Isolation and sequence determination of a cDNA clone related to human cytochrome P-450 nifedipine oxidase. *Proc. Natl. Acad. Sci. USA*, **83**: 8064-8068 (1986).
7) Molowa, D. T., Schuetz, E. G., Wrighton, S. A., Watkins, P. B., Kremers, P., Mendez-Picon, G., Parker, G. A. and Guzelian, P. S.: Complete cDNA sequence of a cytochrome P-450 inducible by glucocorticoids in human liver. *Proc. Natl. Acad. Sci. USA*, **83**: 5311-5315 (1986).
8) Aoyama, T., Yamano, S., Waxman, D. J., Lapenson, D. P., Meyer, U. A., Fischer, V., Tyndale, R., Inaba, T., Kalow, W., Gelboin, H. V. and Gonzalez, F. J.: Cytochrome P-450 hPCN3, a novel cytochrome P-450 IIIA gene product that is differentially expressed in adult human liver. cDNA and deduced amino acid sequence and distinct specificities of cDNA-expressed hPCN1 and hPCN3 for the metabolism of steroid hormones and cyclosporine. *J. Biol. Chem.*, **264**: 10388-10395 (1989).
9) Wrighton, S. A., Brian, W. R., Sari, M. A., Iwasaki, M., Guengerich, F. P., Raucy, J. L., Molowa, D. T. and Vandenbranden, M.: Studies on the expression and metabolic capabilities of human liver cytochrome P450IIIA5 (HLp3). *Mol. Pharmacol.*, **38**: 207-213 (1990).
10) Wrighton, S. A., Ring, B. J., Watkins, P. B. and VandenBranden, M.: Identification of a polymorphically expressed member of the human cytochrome P-450III family. *Mol. Pharmacol.*, **36**: 97-105 (1989).
11) Kitada, M., Kamataki, T., Itahashi, K., Rikihisa, T., Kato, R. and Kanakubo, Y.: Purification and properties of cytochrome P-450 from homogenates of human fetal livers. *Arch. Biochem. Biophys.*, **241**: 275-280 (1985).
12) Westlind, A., Malmebo, S., Johansson, I., Otter, C., Andersson, T. B., Ingelman-Sundberg, M. and Oscarson, M.: Cloning and tissue distribution of a novel human cytochrome P450 of the CYP3A subfamily, CYP3A43. *Biochem. Biophys. Res. Commun.*, **281**: 1349-1355 (2001).
13) Komori, M., Nishio, K., Kitada, M., Shiramatsu, K.,